A STUDY OF MATRIX ISOLATED IONS BY ELECTRON SPIN RESONANCE SPECTROSCOPY

A thesis submitted in partial fulfilment of the requirements for the Degree of Doctor of Philosophy in Chemistry in the University of Canterbury

By A.J. McKinley

University of Canterbury 1985

Except as provided by the Copyright Act 1994, no part of this publication may be reproduced or stored in a retrieval system in any form or by any means without the prior written permission of the copyright owner, A.J. McKinley.

http://hdl.handle.net/10092/9393

A STUDY OF MATRIX ISOLATED IONS BY ELECTRON SPIN RESONANCE SPECTROSCOPY

A thesis

submitted in partial fulfilment

of the requirements for the Degree

of

Doctor of Philosophy in Chemistry

in the

University of Canterbury

by

A.J. McKinley

University of Canterbury

1985

SCIENCES
LIBRARY
THESIS
copy 2

TO MY PARENTS

PUBLICATIONS

The following paper relating to research described in this thesis has been accepted for publication.

"The ESR observation of $^{14}NH_3^+$ and $^{15}NH_3^+$ trapped in an argon matrix at 12K."
A.J. McKinley, R.F.C. Claridge, P.W. Harland
accepted for publication in Chemical Physics.

A reprint of this paper is included inside the back cover of this thesis.

ABSTRACT

The objective of this project was to attempt to trap small molecular ions in an argon matrix and study the structure of these ions using electron spin resonance spectroscopy. To this end an apparatus designed for matrix isolation ESR was developed in a number of stages concurrently with matrix isolation experiments.

Early experiments used conventional electron impact ion sources but these sources were found to be unsuitable for producing ions to trap in an argon matrix due to the energy of the ions. In these experiments problems arose due to contamination of the matrix by methyl radicals and hydrogen and nitrogen atoms which obscured the spectral range of interest that is around g = 2. Vacuum ultra-violet photolysis was used to produce ions and was found to be successful.

The molecular ion NH_3^+ has been trapped in an argon matrix at 14K by photo-ionisation of an NH_3/Ar mixture during deposition. The NH_3^+ cation has been found to be rigidly trapped in the argon matrix and exhibits a powder-type ESR spectrum. The derived magnetic parameters agree well with those obtained by other workers in different matrices. A strong reversible temperature dependence of the linewidth of the NH_3^+ spectrum has been observed.

Argon resonance photolysis of methyl iodide and methyl bromide argon mixtures during deposition was found to produce free methyl radicals in addition to methyl radicals interacting weakly with a high spin nucleus or nuclei. These species have been tentatively assigned on chemical evidence as $CH_3^{\cdot}\cdots I^-$ and $CH_3^{\cdot}\cdots Br^-$ respectively. The complexity of the spectra resulted in complete solution not being possible.

CHAPTER I

Introduction

In the Chemistry Department, at the University of Canterbury, there is a strong interest in gas phase ion chemistry. Structural studies upon ions, however, are quite a difficult problem experimentally as only small concentrations of ions can easily be achieved in the gas phase and consequently only the most sensitive structural probes may be used - for example - spectroscopic studies of the emission from exited ions, where the excitation source is often a laser. Indirect structural information can often be obtained about ions in the gas phase by differences in ion/molecule rate coefficients or product ratios and by measuring enthalpies of formation of ions using photoionisation or electron impact and comparing these values with theoretical calculation of the enthalpy of formation for different possible structures of the ion. Structural information inferred from reactivity is often unreliable as differences in rate coefficients or product ratios between ions from different sources may often only reflect differences in their internal energy.

Matrix isolation offers a relatively simple method of achieving high concentrations of ions for structural studies. There was experience in this department of matrix isolation [BUT71, VRE74]. A rather well equipped electron

spin resonance (ESR) spectrometer and a Displex closed cycle helium refrigerator were available. It was felt these factors could be combined to study the structure of some small molecular ions using ESR via the matrix isolation technique.

At the time this project commenced, early 1981, numerous studies had been reported on unstable neutral molecules using a variety of spectroscopic techniques - for example - infra-red spectroscopy, visible and ultra-violet spectroscopy, electron spin resonance, Mössbauer spectroscopy, Raman spectroscopy and magnetic circular dichroism spectroscopy [BAR81].

There were, however, few investigations of ions using the matrix isolation technique. A summary of the methods used to generate ions in rare gas matrices follows in the review of the literature on page 11.

A matrix isolation experiment involves the formation of a solid matrix at cryogenic temperatures, usually a solidified gas, containing a reactive species of interest, often referred to as a guest. If the matrix is unreactive and has sufficient rigidity, which is a parameter usually controlled by the matrix temperature, diffusion of the guest within the matrix will be minimal. This means large concentrations of the guest can be built up, until a reasonable level suitable for detection by the particular

spectroscopic probe in use, can be obtained. The matrix is generally a rare gas, for example argon, but more reactive gases such as nitrogen and hydrocarbons are in use. The guest under investigation is usually produced in the matrix, after deposition of the matrix gas containing a small percentage of the precursor for the guest. Alternatively, as was the intention in our experiments, the guest may be formed in the gas phase near the surface of the matrix during deposition.

The objective of this project was to trap ions directly from the gas phase, where they had been formed in electrostatic ion sources and where some control over their production could be exercised. This would possibly allow the use of a device to select a particular ion from a mixture. For example, the ion source could be coupled to a quadrupole mass filter, which as well as selecting ions with a particular mass to charge ratio could be used to focus and decelerate the ion beam. The trapped ions would then be detected and their electronic structure probed using ESR spectroscopy.

1.1 INTRODUCTION TO ESR SPECTROSCOPY

ESR spectroscopy is a very suitable technique for matrix isolation experiments as it is very selective, being only sensitive to radicals, and it has a very low detection limit. The detection limit of the Varian E-12 spectrometer

used in this work would be approximately 10^{12} spins for a single 0.1 mT wide line. As most singly charged ions are radicals ESR spectroscopy appeared ideally suited to this project.

ESR spectroscopy involves the determination of the energy difference between the two principal spin states of the unpaired electron in a radical. To remove the degeneracy between these states the radical is placed in a large magnetic field and a microwave source causes transitions between these states. If the radical has a nucleus or nuclei with a magnetic moment the electron spin states are further split by the influence of these nuclei. The energy of an electron in a magnetic field is summarised by expression 1.1:

$$E = h\nu = \beta \vec{B} \cdot \bar{g} \cdot \vec{S} - \beta_n \vec{B} \cdot \bar{g}_n \cdot \vec{I} + \vec{S} \cdot \bar{A} \cdot \vec{I} \quad (1.1)$$

where E = the energy of the particular spin state,

h = Planck's constant,

ν = frequency of the applied radiation,

β = Bohr magneton,

$\vec{B}$ = the magnetic field vector,

$\bar{g}$ = the g operator which gives the interaction between the magnetic field and the electron spin, this operator defines the position of the centre of the resonance and its value gives an indication of the type of orbital

the unpaired electron resides in,

$\vec{S}$ = the electron spin vector,

$\bar{g}_n$ = the nuclear g operator which gives the interaction between the nuclear spin and the magnetic field,

β_n = the nuclear magneton,

$\vec{I}$ = the nuclear spin vector,

$\vec{S}$ = the electron spin vector,

$\bar{A}$ = the hyperfine coupling operator which is the interaction between the electron spin and the nuclear spin,

The second term in the expression 1.1, called the nuclear Zeeman term is small and is usually described as isotropic reducing to:

$$- g_n \beta_n B I_z \qquad (1.2)$$

where the magnetic field is assumed to be along the z axis so only the component of the nuclear spin vector in this direction can interact.

The third term in expression 1.1, the hyperfine interaction term can be expanded into two terms. The first term, expression 1.3a called the Fermi contact term treats the interaction of electric currents caused by the spinning electron and the magnetic moment of the nucleus. This term is isotropic. The second term expression 1.3b the dipolar

term describes the interaction between the magnetic moment of the electron and the magnetic moment of the nucleus. This term is anisotropic and if the unpaired electron is in an s type orbital averages to zero.

$$\frac{8\pi}{3} g\beta g_n \beta_n \, \delta(r) \, \vec{I}.\vec{S} \qquad (1.3a)$$

where $\delta(r)$ = the Dirac δ function and imposes the condition that r, the radial distance between the electron and the nucleus equals zero as $\vec{I}.\vec{S}$ is integrated over all co-ordinates of the electron.

$$-g\beta g_n \beta_n \left[\frac{\vec{I}.\vec{S}}{r^3} - \frac{3(\vec{I}.\vec{r})(\vec{S}.\vec{r})}{r^5} \right] \qquad (1.3b)$$

If the radical containing the unpaired electron is freely rotating the expression 1.1 simplifies to:

$$E = h\nu = g\beta B S_z - g_n \beta_n B I_z + a\vec{S}\cdot\vec{I} \qquad (1.4)$$

where only the Fermi contact term need be considered for the hyperfine interaction as the dipolar term averages to zero.

If the hyperfine interaction, a, is much smaller than the electron Zeeman interaction $g\beta B$, a first order solution of expression 1.4 gives the energy level diagram [CAR67] of an unpaired electron interacting with a nucleus having a spin of 1/2 shown in fig 1.1.

Inspection of expressions 1.3a and 1.3b also shows that

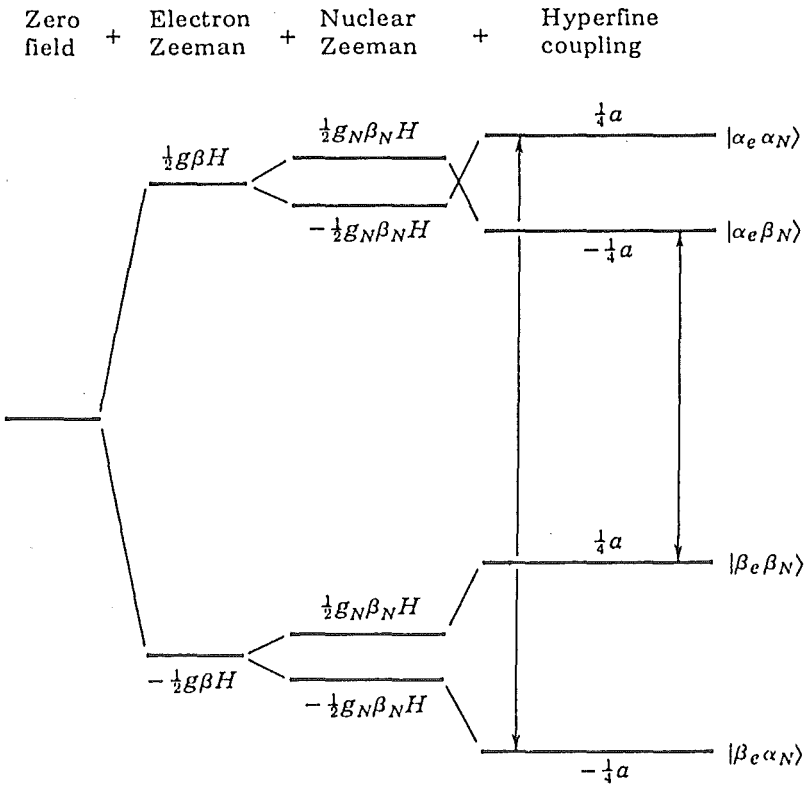

Fig 1.1 Energy level diagram of a radical containing one unpaired electron and interacting with one nucleus having a spin of 1/2. First order isotropic solution of the Hamiltonian.

isotopic substitution of an interacting nuclei for example replacement of ^{14}N by ^{15}N in a radical will result in the magnitude of the hyperfine interaction changing by $g_n(^{15}N)/g_n(^{14}N)$. Values for this ratio are readily available in the literature.

The main disadvantages of ESR spectroscopy, are firstly the experimental difficulties in using the technique - for example - arranging magnetic field modulation at a sample which is under vacuum, as discussed in section 3.1, and secondly that the common contaminants in matrix isolation experiments are radicals. These often occur at about the same g value as the species of interest and therefore mask the signals under observation.

Anisotropic effects resulting in powder-type spectra are often observed in the spectra of free radicals trapped in rare gas matrices. This is because free rotation of the guest radical is often hindered by the matrix, sometimes to the extent that this rotation is slow on the ESR time scale, that is, a period of the rotation of more than 10^{-9} s . The interpretation of powder type spectra involving a number of paramagnetic nuclei may not always be achieved. The theory of ESR spectroscopy and types of spectra observed are well known and can be found in a number of standard texts. [CAR67, WER72, BOX77, POO83]

1.2 REVIEW OF THE LITERATURE

The following review will deal only with the developments of trapping ions in rare gas matrices. The general field of matrix isolation has been reviewed a number of times, the most recent being that of Perutz [PER85].

The first trapped ions to be characterised, in rare gas matrices were the chemically bound pair $Li^+O_2^-$. Andrews [AND68] formed this ion pair during the concurrent deposition of lithium atoms, dioxygen and argon at 15 K. Electron transfer and ion pair formation occurred spontaneously during deposition. Andrews and Pimentel [AND66] had produced similar species with alkali metal atoms and nitric oxide in argon. For the species $M^+O_2^-$, the alkali metal ion was shown by Andrews et al. [AND73] to be closely interacting with the superoxide ion. Vibration spectroscopy indicated that the O_2^- stretching mode is modified by the alkali metal.

Kasai and McLeod [KAI68] produced the first examples of isolated ions in a rare gas matrix. These experiments have been further described in a review by Kasai [KAI71]. Metal atoms such as Na, Cd, Cr and Mn were co-deposited with HI in an argon matrix. Subsequent photolysis with a high pressure mercury lamp caused electron transfer from the metal to the HI molecule, which acts as an electron acceptor. The general reaction scheme is:

$$M + HI \longrightarrow M^{+} + H\cdot + I^{-}$$

ESR spectroscopy was used in these experiments. Except for the experiments in which sodium atoms were used, both the metal ion and the hydrogen atoms produced are observed. In the sodium example neutral sodium atoms are observed and the signal is replaced by the hydrogen atom signal upon photolysis. Super-hyperfine interactions on the metal ion signal, from either the hydrogen atoms, or the iodide ions were not observed in these experiments. Consequently Kasai concluded a spacing of at least 5 angstroms must exist between the metal ion and its counter ion in the matrix.

It is interesting to note that in these experiments the photon energy required to achieve ionisation is well below the ionisation potential of the metal atom in the gas phase. Kasai [KAI71] discussed the energy required for electron transfer (Δ E) in terms of the ionisation potential of the metal, (IP(M)), the electron affinity of the acceptor molecule, (EA(A)), and the spacing between these species. He assumed the matrix, which has a dielectric constant ε, acts only as a cage to contain the resultant ions at a spacing R. The following equation derived by Mulliken [MUL52] may be used to predict the energy required for electron transfer.

$$\Delta E = IP(M) - EA(A) - e^2/\varepsilon R^2$$

Using this equation and a spacing of 7-8 angstroms between the trapped sodium atom, (IP(M) = 5.18 eV), and the HI molecule, electron transfer would be predicted to occur with photolysis using "yellow" light (ΔE = 2.5 eV). This was indeed the experimental observation.

Kasai also applied this method to the formation of molecular anions by replacing the HI molecule with another suitable electron acceptor. In this way the molecular anions of tetracyanoethylene and diborane were produced. Experiments with furan produced a ring-opened anion. Dissociative electron capture was also shown to be a convenient method of producing phenyl radicals from fluorobenzene.

Chronologically, the next technique developed to produce matrix isolated ions, utilised photoionisation of the precursor molecule using vacuum ultra-violet (VUV) radiation, either during or after the formation of the matrix. Initially VUV sources were closed atomic resonance lamps with LiF windows. Either argon or hydrogen atoms excited by a microwave discharge were used as the source of the radiation. In Table 1.1 the energies of some commonly used atomic resonance lamps are listed.

The first trapped ion reported produced by this method was C_2^- trapped in argon. Milligan and Jacox [MIL69]

Table 1.1 Energies and wavelengths of some common atomic resonance lamps [OKA78]

	Energy (eV)	Wavelength (nm)
Helium	21.22	58.4
Argon	11.83 11.62	104.8 106.7
Krypton	10.64 10.03	116.5 123.6
Xenon	9.57 8.44	129.5 147.0
Hydrogen (1% in Helium)	12.09 10.20	102.6 121.6
Mercury	6.71 4.89	184.9 253.7

observed the infra red spectrum of this ion when acetylene in argon was photoionised using a hydrogen resonance lamp. This method has been extended to open tube discharges generally using argon, where direct reaction with ions and metastables from the discharge is possible.

Photoionisation has become a popular source of matrix isolated ions and many examples of its use can be found in the literature. For instance intensive investigations of the halomethyl ions produced by photo ionisation of halogen derivatives of methane in argon matrices has been reported by Andrews et al.[AND79] and Jacox [JAC78].

Irradiation, using a high energy (2 keV) proton beam from a radio frequency accelerator, of a CCl_4 argon mixture during deposition was used by Andrews et al. [AND75] to produce CCl_3^+ as well as CCl_4^+ and Cl_3^+ trapped in the matrix. Low energy electron bombardment during deposition was used by Milligan et al. [MIL70] to produce NO_2^- trapped in an argon matrix.

Salt-like ion pairs have also been produced in matrices by the simultaneous deposition of a salt vapour and a Lewis acid. Ault and Andrews formed the ion pair $Na^+Cl_3^-$ when NaCl vapour and HCl gas were condensed in argon. [AUL75]

This was the stage of development of "ionic" matrix isolation at the beginning of this project.

There were no clear examples of isolated ions formed in the gas phase being trapped in matrices. The photoionisation method for cation production offered little control over the final product. For instance, the product of VUV photolysis of acetylene argon matrices with a hydrogen resonance lamp, had been shown to be C_2^- [MIL69]. This ion was produced according to Brus and Bondybey [BRU75] by electron transfer from an acetylene molecule to C_2, which had been formed from another acetylene molecule which had been stripped of its hydrogen atoms.

Most of the matrix isolation studies up to this time had used argon as the matrix gas. The main exception to this was when multiple trapping site effects were investigated. Using a series of rare gases, it was possible to vary the cage size in a systematic manner. Argon was probably the most commonly used matrix gas owing to its low cost and convenient freezing point (83.3 K). A reasonable temperature for an argon matrix experiment is 10 K which was easily achieved with liquid helium and later with closed cycle helium refrigerators.

Bondybey and English noted [BON79] that neon appeared to be a better host than argon for trapping ions although lower temperatures are required, usually below 6 K. Diacetylene cations trapped in argon matrices were found to have broad shifted electronic spectra compared with the same

cation trapped in neon matrices whose electronic spectra closely resembled gas phase results. The origin of this effect was ascribed to charge transfer between the matrix and the ion. Bondybey and English suggested that although it is convenient to consider the ionisation potential of argon and the electron affinity of the guest as the controlling parameters in this effect, one should really consider the energy of the conduction band in solid argon and the electron affinity of the trapped cation.

It appears, however, that complete transfer of an electron to the trapped ion which would be the case if the conduction band energy was the controlling factor is the extreme case and a significant charge transfer would be expected to occur at lower energy. The energy of the first exciton in solid argon which is the lowest energy for the formation of a stable argon ion electron pair is 12.1 eV [BAL62]. This is below the energy of the conduction band and would be expected to be at a higher energy than the onset of significant charge transfer between the host matrix and the guest cation.

A variation of the photolysis production of ions trapped in rare gas matrices was introduced by Kelsall et al. [KEL82] who observed the production of large aromatic ions trapped in argon matrices after two photon ionisation. A high pressure mercury lamp was used to photoionise napthalene in an argon matrix. It was shown that ionisation

proceeded from the formation of a long lived excited state followed by absorption of a second photon.

The most recent advances in "ionic" matrix isolation have come from the experiments of Knight et al. Using an open tube neon discharge and a neon matrix at 4 K, Knight and Steadman [KNI82] were able to observe the formation and trapping of NH_3^+ and CO^+ by ESR spectroscopy. In the course of that work, trapped ions formed by ion molecule reactions between CO^+ and CO or N_2, giving $C_2O_2^+$, and N_2O^+ respectively, were observed. In a development of the electron bombardment of the matrix, Knight et al. [KNI83] produced N_2^+ by low energy electron bombardment of a nitrogen argon mixture during deposition. Knight et al. found it was necessary for the deposition target to be held at a positive potential of at least 60 V above the electron source for cations to be produced trapped in the matrix. He assumed this was due to some form of space charge effect.

Knight et al. [KNI84] also used fast atom bombardment (FAB) to produce ions trapped in neon matrices. A beam of excited neon atoms was directed at grazing incidence towards a metal surface and then onto the matrix deposition target. Cadmium ions were formed in the neon matrix. Neon FAB of gases, for example CH_4, was also able to produce ions trapped in the resulting neon matrix. Knight suggested that the use of a heavier atom for the FAB source and a separate source of the neon matrix gas should increase the sputtering

yield.

In an earlier report Knight et al. [KNI83] reported preliminary experiments performed using a mass selected cation beam and a neon matrix. Knight noted this arrangement was a feasible method of producing ions trapped in a neon matrix but he was having difficulties optimising the experimental parameters.

1.1 GENERAL INTRODUCTION TO EXPERIMENTAL APPARATUS

The experimental apparatus used in this project was developed in two sections.

The first section developed was the apparatus for ion generation. The development of this apparatus is described in Chapter III. This development consisted of operating the ion source in a vacuum system and establishing its general operating behaviour and performance. As a part of this process a brief study of the visible emission from this source was conducted and an investigation of the possibility of observing ions by ESR directly in the gas phase conducted.

The second section was the apparatus for performing ESR experiments and the matrix isolation process. This section of the apparatus is described in Chapters IV, V and VI. Initially, an ESR apparatus designed for single crystal studies was intended to form the basis of this section of the

apparatus. Various experiments were performed with this apparatus to verify it was working correctly and some improvements were made. This apparatus was then combined with the ion source and matrix isolation experiments attempted. These experiments were unsuccessful and a different design of ion source was tried. These experiments were again unsuccessful and photolysis with vacuum ultra violet radiation was tried to produce ions. This method was found to be successful, however further problems were found with the ESR matrix isolation apparatus and a new apparatus was designed and constructed.

CHAPTER II

ION SOURCE DEVELOPMENT

The ion source chosen for this project was a charged particle oscillator ion source (CPO). This ion source was designed by McIlraith [MCI66] following theoretical studies of electron paths in an X-ray tube. McIlraith's design was improved by Fitch et al. [FIT70] and the performance of this ion source investigated by Rushton et al. [RUS71]. This particular type of ion source was chosen as it could produce very high ion beam densities. An ion source for this work was obtained from McIlraith.

2.1 OPERATION OF THE CHARGED PARTICLE OSCILLATOR ION SOURCE

An ion source generally relies on electron-neutral collisions to generate ions which are then accelerated out of the collision region and focussed into a beam. The current density of the resultant ion beam is limited by the frequency of the electron-neutral collisions and this is a function of the gas pressure within the source and the electron current. In a simple ion source, such as the Extranuclear model 041-3 shown in fig 2.1 electrons are generated from a thoriated tungsten filament and accelerated across a collision region to an electron trap. The positive ions produced are repelled by an element held at positive potential and accelerated by

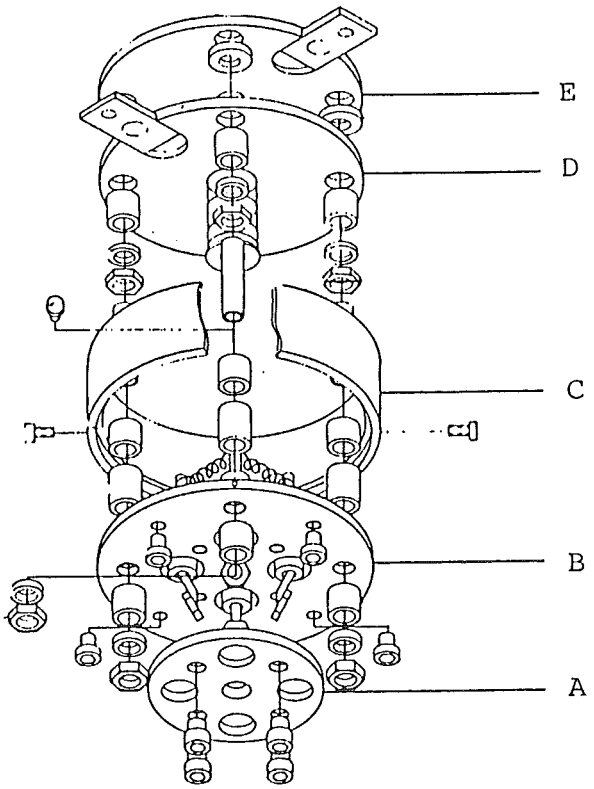

Fig 2.1 Diagram of the Extranuclear Laboratories Inc. model 041-3 ion source. A aperture plate, B filament plate, C filament shield, D ion region plate, E Extractor plate. [EXN75]

an extractor lens.

The principle of operation of the CPO ion source is rather novel. Until McIlraith's development work on this ion source, it had been generally accepted that a moving charged particle could not be confined in a closed volume in just an electric field. [MCI66]

The CPO ion source which is shown in fig 2.2 consists of a stainless steel tube in the centre of which are two tungsten wires. The wires are fixed in place by insulating plates which fit over the metal end plates of the tube. The wires fit through clearance holes in the conducting plates and then through small holes drilled about the centre of the insulating plates. A positive potential, generally between 2 and 5 kV, is applied between the central wires and the tube. Spontaneous ionisation of a molecule in the source produces an electron which is accelerated towards the central wires, passing between them. This electron is then decelerated by the electric field at the surface of the tube and attracted back to the wires. The trajectory followed by the electron is in the form of a figure eight and may be up to several kilometres in length. This electron collides with further gas molecules and produces more electrons and positive ions. The positive ions are accelerated towards the surface of the tube and upon striking it form more electrons. A slot cut in the centre of the tube wall allows a beam of positive ions to leave the source. It is necessary to have

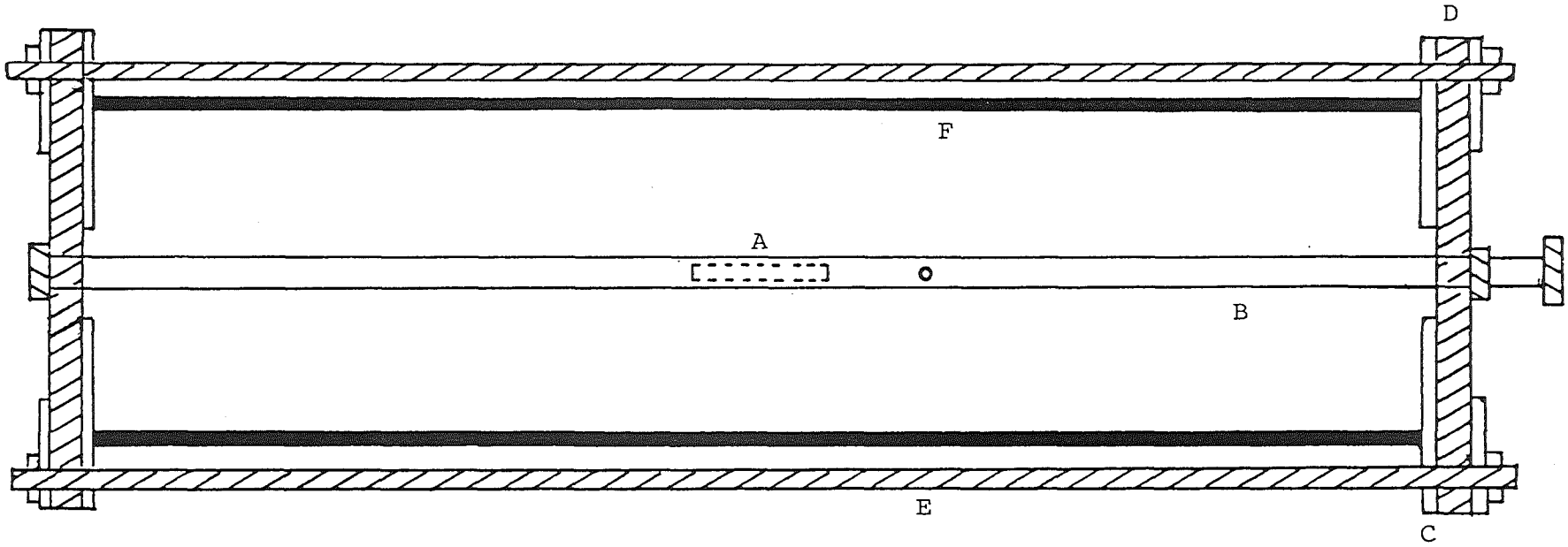

Fig. 2.2 Schematic diagram of charged particle oscillator ion source. A position of ion beam aperture , B Anode wires, C Metal end-plates, D Insulating end-plates, E brass rods, F Cathode tube.

conducting end plates to minimise end-effects upon the electron trajectories.

The ion beam consists of high energy positive ions, the energy distribution having two peaks one at 0.36 and the other at 0.75 of the applied potential [KHO77]. These energy peaks are presumably due to the probability of ionisation being significantly higher at particular radial distances out from the wires. Consequently as the accelerating potential experienced by the ion will be a function of its radial position the final ion energy will be a function of the position of its formation. Excited neutral molecules and electrons trapped by space charge effects are also present in the beam. The beam is visible due to emission from excited species. Without focusing, the beam follows the solid angle subtended by the slot in the direction perpendicular to the axis of the cylinder and diverges only slightly about the other axis.

The advantage of this ion source is that high beam currents can be achieved even at low pressure. This is because the probability of ionising electron-neutral collisions within the source is much more likely than in a conventional ion source because of the extended electron trajectories.

2.2 TESTING OF THE CHARGED PARTICLE OSCILLATOR ION SOURCE

The ion source was tested in an all glass vacuum system. The vacuum system consisted of a glass bell jar, pumped by two three-stage water cooled glass oil diffusion pumps. The ion source was mounted on a stainless steel flange which formed the top of the bell jar. The gas to be ionised was fed to the ion source through a needle valve and a stainless steel capillary connected to the side of the ion source. To measure the ion beam current a 25 mm square plate of stainless steel was placed in the ion beam and a wire attached to this plate brought out through the flange by an insulated feedthrough to a micro-ammeter. The main voltage for the ion source was introduced through another feedthrough. Initially the ion source was powered with a transistorised inverter supply (Spellman model RHR5PN30/FG). This supply provided 0 - 5 kV at up to 10 mA. This supply has a high output impedance which is necessary as the ion source becomes a negative resistor during operation. The pressure in the bell jar was measured with an ion guage.

The first experiments were made using mainly nitrogen gas through the ion source. The general behaviours of the ion current versus pressure and source voltage characteristics were studied qualitatively and found to be in accord with extensive studies by Rushton and Fitch [RUS71] and Rushton et al. [RUS73]. They noted that the ion source would operate in two modes, the oscillating mode, as described above, at low

pressures and another mode at higher pressures. In the second mode termed the orbiting mode, the ionising electrons within the source move in circular orbits around the central wires. This mode is characterised by operating voltages less than 1 kV and low ion beam currents. In the oscillating mode ion beam densities of around 0.1 mA cm^{-2} were recorded for nitrogen source gas and an applied voltage of 5 kV. The highest beam currents were observed at the lowest pressures, however the source voltage required is inversely proportional to the source pressure which means the maximum beam current is limited by the maximum available source voltage.

The Spellman supply that was used initially to power the ion source was on loan so it was necessary to build a replacement supply. For simplicity a conventional direct mains powered supply was chosen. This supply was constructed using a 240 to 3.3 kV transformer, the output of which was full-wave rectified and then filtered with a bank of high voltage capacitors. The output voltage was varied using a "Variac" which controlled the input voltage to the transformer. A resistance ballast was required in series with the ion source owing to the low output impedance of this supply.

As mentioned above the ion beam from the CPO ion source is visible due to emission from excited species in the beam. A preliminary study of this emission was undertaken. A silica window was mounted in the side of the bell

jar in line with the ion beam. The emission from the beam passed through this window and a vibrating reed chopper into a model 218 0.3 m McPherson monochromator equipped with an EMI 9558QB UV photo-multiplier. The output of the photo-multiplier was amplified by a model 129A PAR lock in amplifier and recorded on a chart recorder.

The highest emission output was found when the ion source was operated with reverse polarity using nitrogen as a source gas. In this mode the ion source operates as a high energy electron gun. Emission bands corresponding to the first positive series of nitrogen and the first negative series of nitrogen ions were observed. [PEA76]

In the course of these experiments two problems were encountered with the CPO ion source. The first problem was a general dielectric breakdown in the ion source chamber when high voltages were applied to the source. The ion source produced high concentrations of stray ions in this chamber which promoted breakdown. When the high voltage supply to the ion source was completely surrounded by earthed braid dielectric breakdown did not occur. The second problem was caused by sputtering of metal from the tube walls onto the insulating end plates which caused tracking across them. One of the insulating plates was made initially from glass, which is not a particularly good insulator for high voltages and after problems with tracking this plate was replaced using machinable glass ceramic (Macor) which

is a better insulator. Also as the new insulating plate was easily machined it was possible to fashion it in such a way as to minimise tracking. Fig 2.3 shows the new design of this insulator.

2.3 GAS PHASE ESR STUDIES

An attempt to observe ions in the gas phase directly with ESR using this ion source was carried out. A disadvantage of the CPO ion source is its sensitivity to magnetic fields. The trajectories of the electrons within the source are distorted by small stray magnetic fields and the high efficiency of the source is lost. Field strengths, as low as a few Gauss, perpendicular to the axis of the source are sufficient to reduce the efficiency of the source [RUS71]. In fact Rushton and Fitch found if the ion source is operated below 10^{-5} Torr the earth's magnetic field influences the operation of the ion source.

The magnetic field at a point 35 cm from the centre of the spectrometer magnet poles was measured using a model 640 Bell incremental gaussmeter (Hall effect). With a main field of 0.35 T the stray field at this position was 5 mT. A piece of 3" steel steam pipe was found to reduce the stray field at this position to 0.015 mT. It was decided to use a combination of steel pipe and mu metal to shield the source, as calculations showed insufficient mu metal was available to perform the whole task.

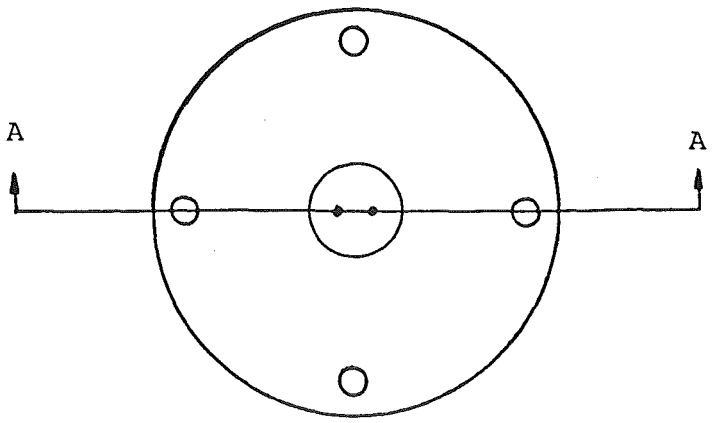

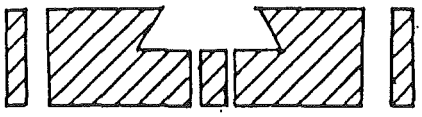

Section AA

Fig. 2.3 Diagram of new insulator for CPO ion source, material Macor.

Several layers of mu metal were wrapped around the source and the glass bell-jar in which the source was placed was surrounded by a length of 7" diameter steel steam pipe. This assembly was bolted to the yoke of the magnets about 35cm from the cavity. Such elaborate shielding was required as it was necessary to operate the spectrometer magnets up to 1 T. High field strengths are necessary due to the low g factors of radicals in the gas phase. The ESR spectrum of the J = 3/2 state of nitric oxide with an X band spectrometer occurs at 0.86 T.

The ion beam flowed down a length of 1" diameter silica tube through a Varian E-235 cylindrical cavity operating in the TE012 mode and then to a 2" diffusion pump. The ion source chamber was independently pumped by another 2 " diffusion pump. Fig 2.4 shows a photograph of the CPO ion source and vacuum chamber. The tuning of the spectrometer was optimised using the ESR signal of a small pressure of nitric oxide gas which had been added to the vacuum system.

No ESR signals attributable to positive ions were observed in these experiments. Argon, nitrogen, carbon dioxide, hydrogen, helium and methane were tried as source gases. It was concluded the concentration of the ions was below the detection limit of the spectrometer. Two other phenomena however were observed.

Fig 2.4 Photograph of the CPO ion source and vacuum chamber used in the gas phase ESR and matrix isolation studies.

2.4 CYCLOTRON RESONANCE PHENOMENA

If an electron is placed in a magnetic field with an oscillating electric field perpendicular to this field, at a particular ratio of the frequency of the electric field to the intensity of the magnetic field the electron will absorb energy from the electric field and be accelerated in a circular orbit. This absorption is called cyclotron resonance and its frequency is governed by:

$$v = (e/mc).B$$

where v = the cyclotron frequency,

e = the charge of the electron,

m = the mass of the electron,

B = the intensity of the magnetic field,

c = the speed of light.

Cyclotron resonance occurs at $g = 2.0$.

In an ESR experiment the sensitivity is controlled by the magnetic dipole moment of the electron, in an electron cyclotron resonance (ECR) experiment the sensitivity is controlled by the effective electric dipole moment of the electron. As the electron dipole moment for an average radius of 0.01 mm is approximately 10^7 times larger than the magnetic dipole moment of an electron, the detection limit of an ECR experiment is 10^7 times more favourable than an ESR experiment [MOT72]. In other words less than

As well as this, all electrons contribute to the ECR signal not just the statistical excess in one spin state, as is the case in an ESR experiment.

10^3 electrons would be sufficient to produce a signal with a typical ESR spectrometer.

Two effects were observed when ESR experiments were conducted using the ion beam from the CPO source. We believe both effects to be cased by ECR.

With the ion source off and a pressure of around 10^{-3} Torr in the cavity, dielectric breakdown was observed in the region around g = 2 with the microwave power above 5 mW. Visible emission was seen from inside the cavity and the noise level of the spectrometer increased markedly. A typical recording of this effect is shown in fig 2.5. The threshold for this effect is proportional to the pressure and the microwave power applied to the cavity. Near the threshold level, the effect occurs in two bands spaced symmetrically around g = 2. As the pressure is raised, or the microwave power is increased, the widths of these bands increase, and merge together. Further increase in power continues to broaden the composite band. This effect was observed with air, nitrogen and argon.

Brown [BRO66] has put forward an explanation of the effect which relies on the rate of electron loss from the cavity as a function of pressure and electron energy. Brown's analysis views this effect at constant field and variable microwave frequency and examines this effect as a function of pressure. For dielectric breakdown to occur a

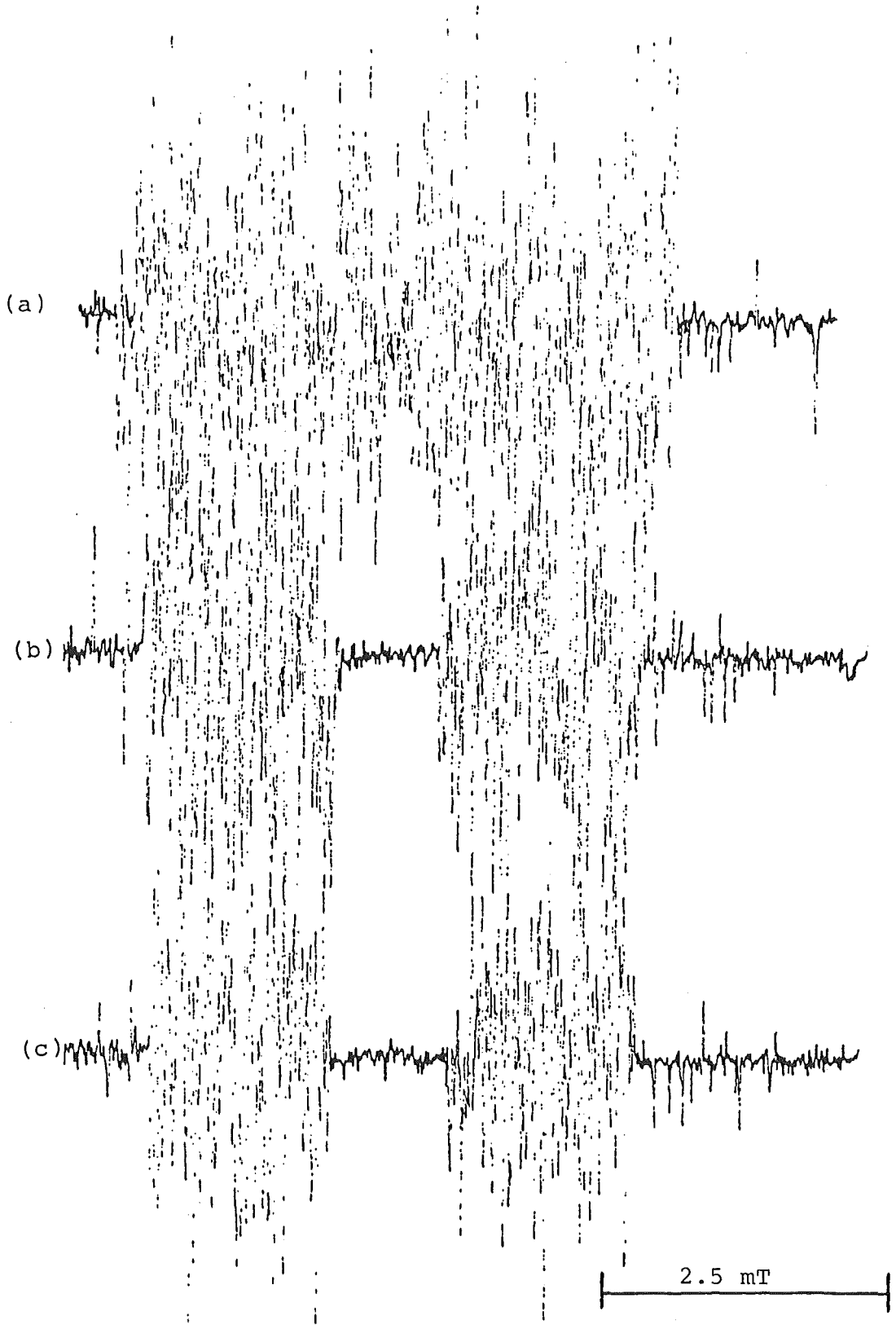

Fig. 2.5 Typical spectrum recorded of dielectric breakdown of argon in the cavity showing effect of increasing microwave power. (a) 5 mW, (b) 6 mW and (c) 7 mW.

steady state condition will develop in which the rates for electron production in the discharge are equal to or exceed the rates of electron loss processes. The low microwave powers required for breakdown imply the rate of electron loss from the cavity is low.

In fig 2.6 reproduced from Brown's book the general absorption profile of pressure verses field is shown as is a graph of the frequency of ionisation (rate of electron production), V_p plotted against electron energy for various pressures. A function, of arbitrary form, for the electron loss rate is added (V_l), the form of the function is a non-linear dependence on the electron energy. At very low pressures below p_0 no breakdown occurs. Above p_0 breakdown occurs and the steady state condition ($V_l <= V_p$) can be achieved between two values of electron energy. As the electron energy in the discharge at a particular field is a function of difference between this field value and the field at g = 2 this band of suitable electron energy will correspond to field bands on either side of g = 2. As the pressure increases the band of suitable electron energy increases until at above p_1 this band is only bounded at the low energy side. The pressure dependence then of this breakdown phenomenon will show at low pressures two bands around g = 2 and as the pressure is increased the bands will merge although the high field and low field limits of these bands will only change slightly.

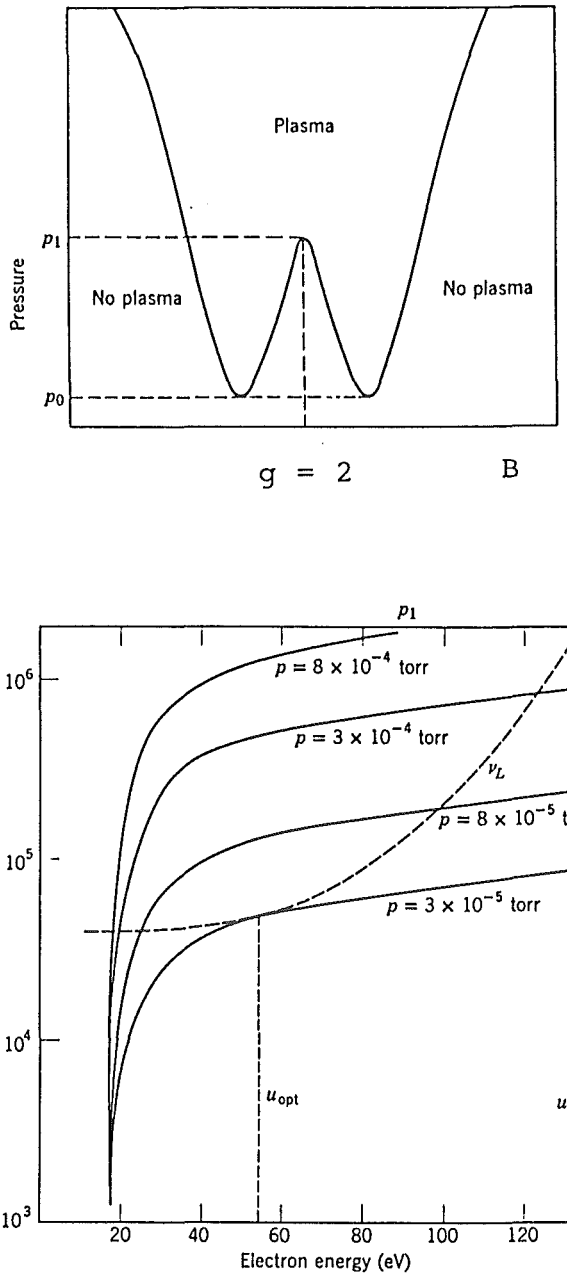

Fig. 2.6 (Upper) Microwave breakdown expressed as a function of magnetic field vs pressure in the cavity. (Lower) Frequency of ionisation as a function of electron energy in a microwave cavity in a magnetic field. Reproduced from Brown [BRO66].

The second effect, also occurring around g = 2, was observed only in the presence of an ion beam passing through the cavity. Three relatively sharp absorptions were observed, rather than the bands of noise seen in the previous effect. The effect was seen when ion beams were formed from the following gases, argon, nitrogen, carbon dioxide, hydrogen, helium or methane. The signal was shown to be dependent on the applied microwave power and the pressure within the cavity. The signal was also shown to be dependent on the voltage applied to a collimator between the ion source and the cavity. Spectra showing the effect of the applied microwave power and the voltage applied to the collimator are given in figs 2.7 and 2.8.

While insufficient ions are present for ESR detection, the observation of electron cyclotron resonance, as discussed earlier, requires only about 10^3 electrons. It appears likely then that this effect is caused by electrons trapped by space charge effects in the ion beam. A positive voltage on the collimator would tend to remove electrons from the ion beam and decelerate the ions until all the ions are repelled. Although some electrons would be accelerated and pass the collimator, most would not reach the cavity. Obviously this effect is not chemical in nature and it seems likely it involves some non-linear interaction of the electron and the microwave magnetic and electric fields within the cavity. Possibly though the cause of this effect may be similar to that of the breakdown effect discussed previously. This

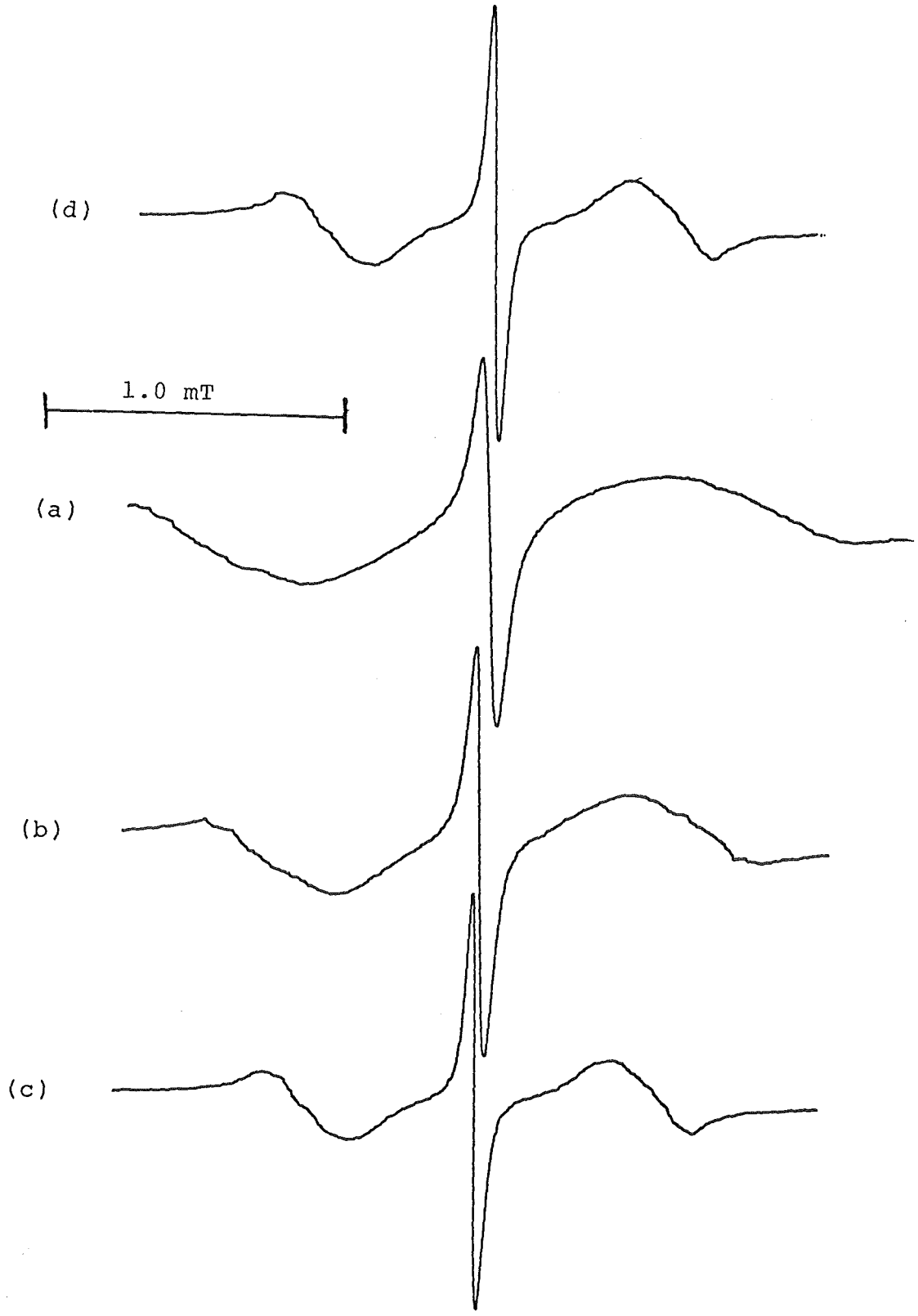

Fig. 2.7 Effect of applied microwave power on the ECR signal. CO_2 ion beam. (a) 0.2 mW (b) 0.05 mW (c) 0.01 mW (d) 0.005 mW.

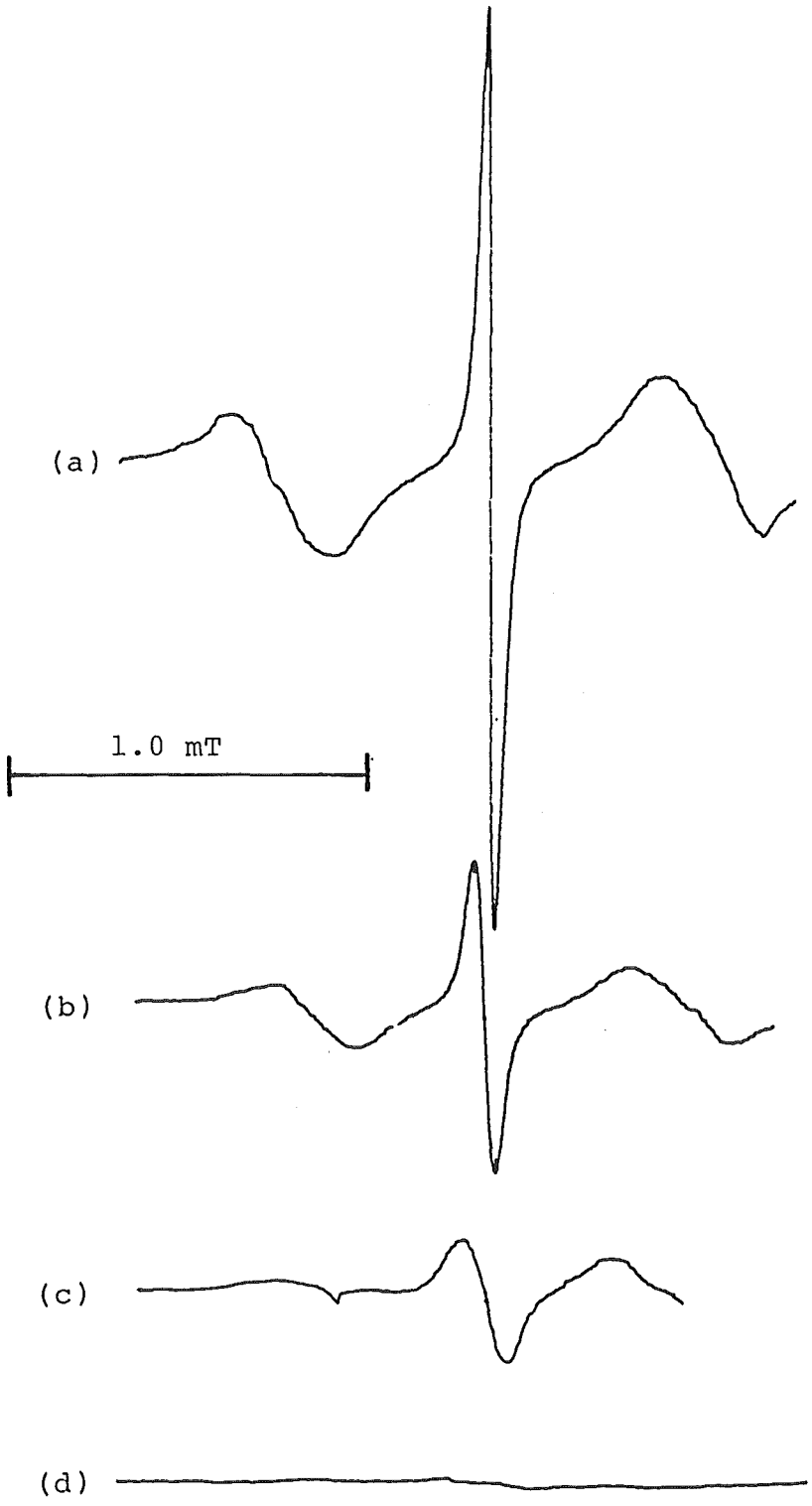

Fig. 2.8 Effect of retarding potential applied to a collimator on the ECR signal. Argon ion beam.
(a) 0 v (b) + 4 kV (c) + 6 kV (d) + 8 kV

effect has been observed previously and noted in the literature. A review by Bradley and Metcalfe [BRA78] of the explanations proffered for origin of this effect concluded none of these explanations were satisfactory.

CHAPTER III

DEVELOPMENT OF THE ESR APPARATUS

An updated version of a low temperature single crystal system designed by Perlson and Weil [PER75] had been constructed in this department. The system had been modified to reduce the number of individual parts and to allow irradiation of the sample at low temperature directly from the front of the apparatus while in the cavity. A series of photographs of this apparatus disassembled is shown in figs 3.1 to 3.4. It was intended that this apparatus be the basis of the system used for matrix isolation so it was necessary to establish that this apparatus functioned correctly and was indeed suitable for matrix isolation experiments.

3.1 GENERAL CONSIDERATIONS

The requirements considered necessary for successful ESR matrix isolation experiments with ions were,

(a) the ability to obtain reproducible and reasonable ESR data

(b) high sensitivity

(c) high vacuum

Fig 3.1 Upper. Side view of the top of the CS202 Displex closed cycle helium refrigerator. Lower. Side view of Displex shroud and attached rotation scale.

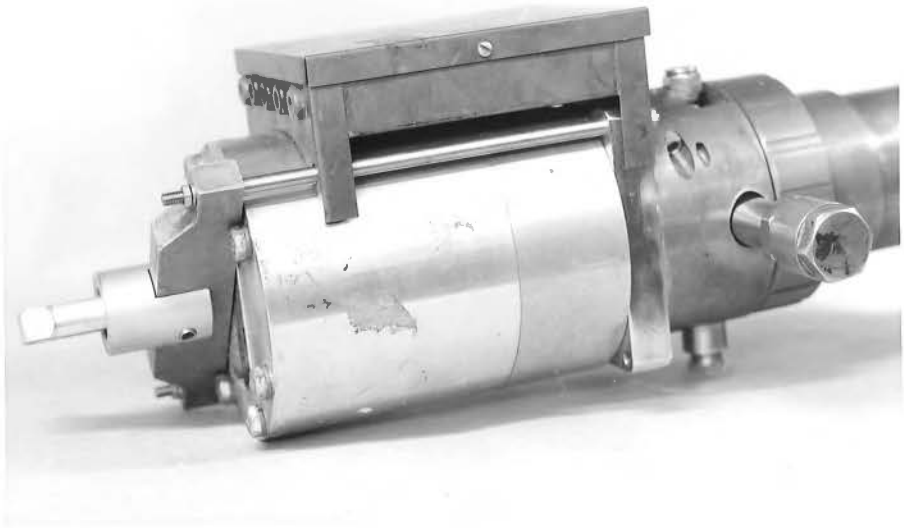

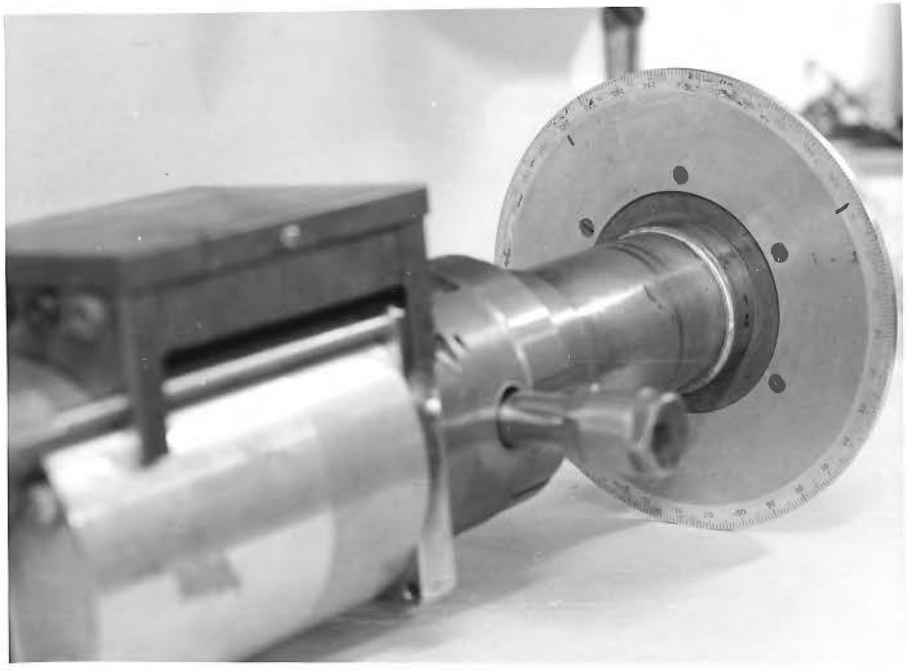

Fig 3.2 Upper. Side view of the Displex shroud and crystal mounting assembly. Lower. Supporting plate with vernier for angular measurement and pistons to lift Displex.

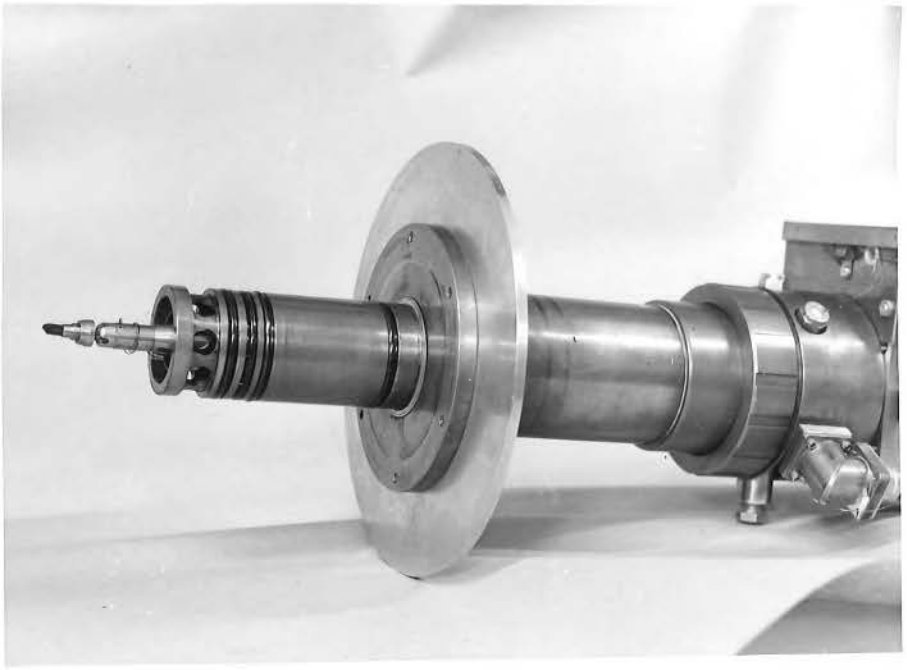

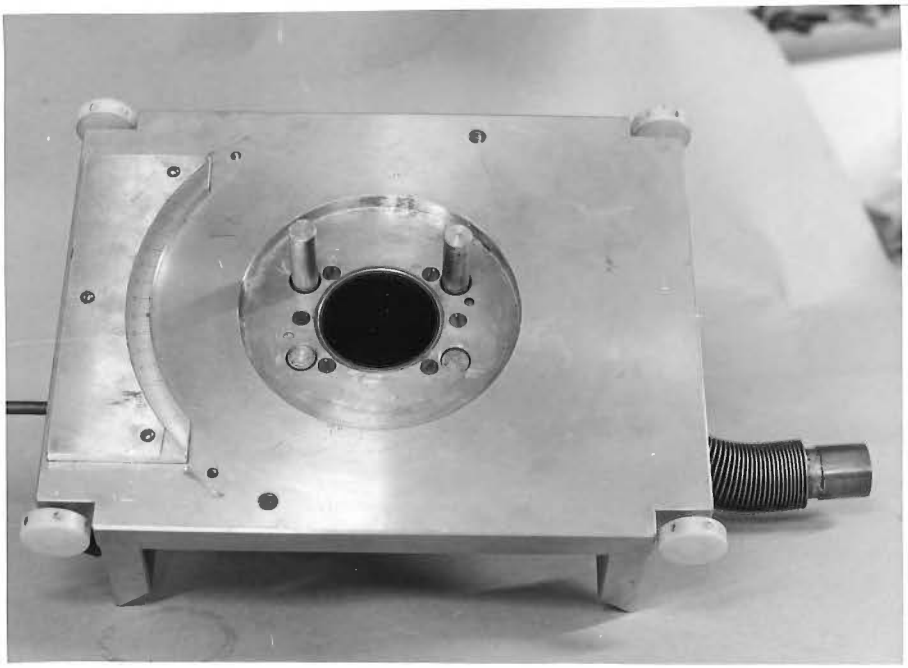

Fig 3.3 Upper. View from underneath the supporting plate showing the brass block which houses the lifting pistons and the Displex assembly slides in. Lower. The Delrin block which holds the modulation coils and the screwdriver for adjusting the orientation of the crystal.

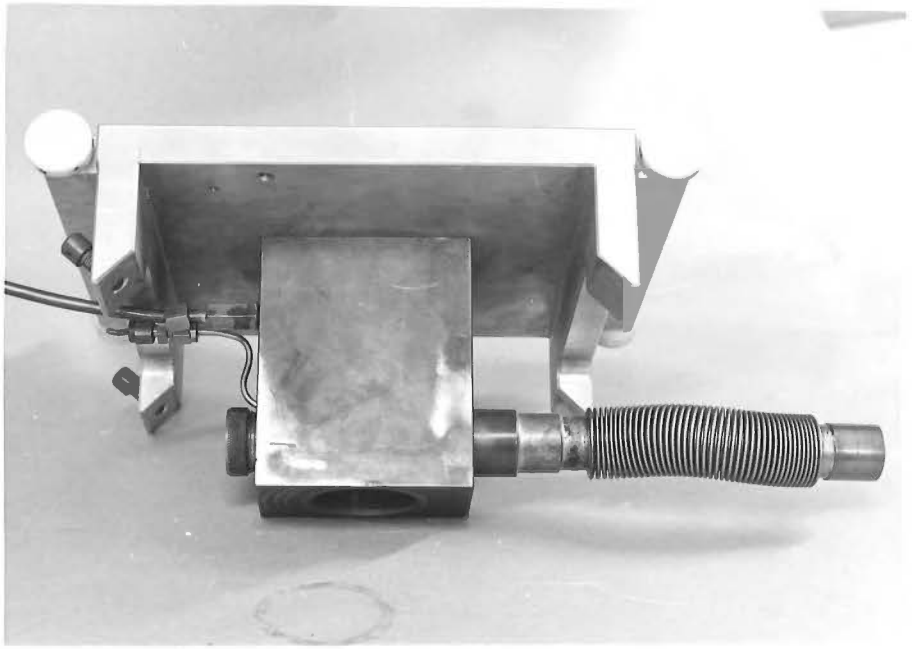

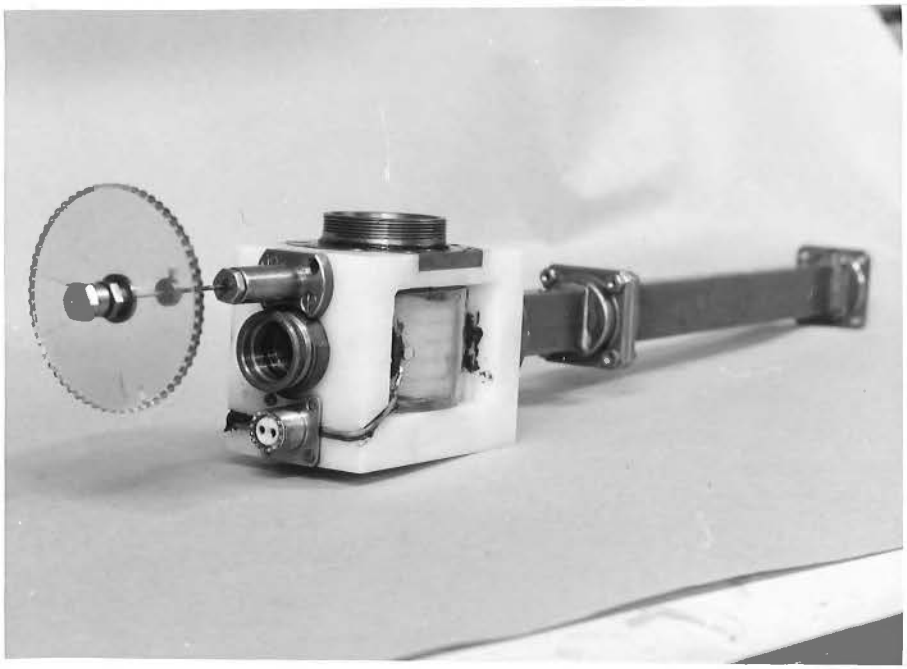

Fig 3.4 Upper. Cavity assembly showing the cavity cup, iris, iris coupling screw and the slot across the top plate of the cavity cup for the screwdriver. Lower. View of assembled apparatus in place between the spectrometer magnet poles.

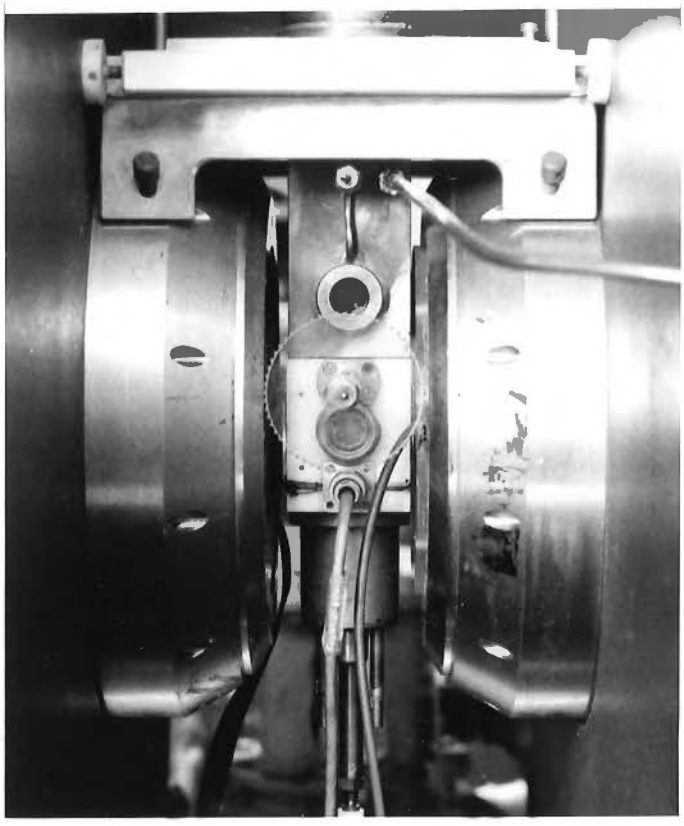

High sensitivity was considered necessary as we expected to achieve only low concentrations of ions in our experiments. High vacuum was required to minimize the effect of neutral contaminants.

The solution of the Hamiltonian for a single isotropic ESR resonance is:

$$h\nu = g\beta B_{eff}$$

where h = Planck's constant,

ν = the spectrometer frequency,

g = the g factor,

β = the electronic Bohr magneton,

and B_{eff} = the resonance field.

The fundamental parameter of an ESR experiment is the g value of the radical under study. To determine g values accurately, the value of the magnetic field, B_{eff}, at the sample and the microwave frequency, ν, at resonance must be known accurately. A detailed discussion of precise g value measurement is presented by Frait and Gemperle [FRA77].

The microwave frequency was measured with a model 6016 Systron Donner electronic frequency counter. This counter measured the frequency directly via a transfer oscillator and was accurate to at least 0.01 ppm.

The measurement of the magnetic field at the sample was more difficult. The magnetic field at the sample may be determined by placing a radical of known g value alongside the sample. However, for accurate measurements the standard must be as close as possible to the sample so conditions at the sample are duplicated at the standard. As low temperature experiments were intended this approach was not really feasible.

An NMR probe, consisting of a small glass tube filled with dilute $CuSO_4$ solution surrounded by the tank coil of a marginal oscillator was mounted to one of the poles of the magnet. The frequency of the NMR transition of the protons in water could then be measured and the magnetic field determined. The gaussmeter used was a modified Micro-Now Instrument Co. model 515. The sensitivity of this gaussmeter had been improved by the addition of an amplifier in the X axis and an amplifier and low pass filter in the Y axis. The 2 kHz low pass filter in the Y axis, a standard Butterworth design four pole filter, removed the noise on the NMR signal caused by the computer. The cut-off frequency was optimised by experiment. The circuit diagram is given in Appendix II.

The field probe was mounted in a perspex holder which fitted into a perspex disc screwed to one of the poles of the magnet. In this way the positioning of the probe was precise and reproducible and different probes could be exchanged for different field ranges. The probe normally in use covered

the range from 0.2T to 0.4T. With this probe permanently fixed, it was then only necessary to measure the offset between this probe and a similar probe which could be placed in the cavity, instead of the sample. The offset measured at 0.33 T was 0.030 mT. and at 0.34 T the offset was 0.037 mT. The offset was not constant. In this work a linear approximation was used. Species of high anisotropy would require a closer examination of the offset dependence.

As the error in the measurement of the microwave frequency was small, the major error in determining the g value came from systematic errors involved in the measurement of the magnetic field at resonance. To test the reproduciblity of the magnetic field measurement crystals of Fluoranthenyl$_2^+PF_6^-$ (FlPF) were synthesised [SAC82]. A description of the synthetic method is given in Appendix I. These crystals had an ESR linewidth of 15mG. The ESR spectrum was recorded with a number of magnetic field markers on a 0.4 mT wide scan and the magnetic field of the resonance was determined from different pairs of markers. The maximum deviation between the highest and lowest field values calculated for the resonance was 0.002 mT. A g value could therefore be expected to have an error of less than $\pm$ 3 ppm. Larger scan ranges lower the accuracy of the positioning of the markers, but this can be countered by slower scanning of the spectrum.

A slight inaccuracy was introduced into these experiments as even with small crystals the resonance of the F1PF crystals was so intense as to temporarily swamp the spectrometer and cause a large shift in the microwave frequency. At resonance the absorption by the crystals is probably sufficiently great to destroy the Q of the cavity which would cause the klystron automatic frequency control (AFC) with the resonant frequency of the cavity and pull the klystron frequency randomly. Once past the resonance the spectrometer frequency returned to very close to its original value and at the end of the scan was practically identical to the initial value.

3.2 CAVITY DESIGN

In an ESR experiment it is necessary to detect absorption of a radio frequency signal by electrons in a magnetic field. Early spectrometers used transmission methods. However, these methods suffer from the problem of detecting a small change in a large signal. The approach used by all modern commercial spectrometers involves a reflection method, described below. As direct current (DC) amplification techniques are inherently inferior to alternating current (AC) techniques the ESR signal is normally amplified as an AC signal. Two main AC approaches have been used. The first, the superhetrodyne technique is expensive and difficult to implement, although it has definite advantages. This technique is discussed by Poole

[P0083]. The other approach, which is the method used by most commercial spectrometers, uses AC modulation of the ESR signal which is amplified by lock-in amplifiers. The Varian E-12 spectrometer described below, which was used in this project, detects the ESR signal by a reflection method and uses lock-in amplifiers.

The sample is placed in a resonant microwave cavity and the microwave power reflected from the cavity is balanced with the microwave power absorbed in the cavity. This is accomplished using an iris coupling screw which changes the amount of microwave power coupled to the cavity. In this way any slight change in the microwave power absorbed in the cavity can easily be detected. This cavity is placed in a large DC magnetic field arranged to be perpendicular to the microwave magnetic field in the cavity. Superimposed on this DC magnetic field is a small AC magnetic field. As any ESR absorption within the cavity will be field dependent, the imbalance signal from the cavity will be modulated at the frequency of the AC magnetic field. This frequency is called the modulation frequency. The imbalance signal which is the ESR signal is amplified over a narrow frequency range around the modulation frequency and the signal is passed through a phase sensitive detector. In this way noise is minimised as the only signal passed must be at the same frequency as the modulation frequency and in phase with it.

When the sample is under vacuum, provision of

modulation at the sample is not straight forward. Modulation is usually provided by Helmholtz coils on either side of the cavity. If the cavity is also under vacuum and the modulation coils are outside the vacuum system, the walls of the vacuum system must allow the modulation field to pass. This is not possible unless the walls of the vacuum system are thin and poor conductors. A non-conductor Delrin (Dupont) is used in the single crystal system of Perlson and Weil [PER75]. Lowering the modulation frequency has the same effect, but as the sensitivity of the spectrometer is a function of the modulation frequency this is not really desirable. In practice as high a frequency as possible is chosen. The ability of an AC magnetic field to penetrate a conductor is controlled by the skin depth which is inversely proportional to the conductivity of the conductor. The skin depth at 100 kHz for copper and brass is 0.2 mm and 0.4mm [POO85].

Modulation may also be generated by vertical posts in the cavity or by placing the modulation coils in the vacuum system. Neither of these methods are particularly satisfactory. The post method results in a large reduction of the Q of the cavity and the maximum modulation amplitude available is quite limited. Placing the modulation coils inside the vacuum systems requires some arrangement to cool the coils if high modulation is used. The other approach is to place the vacuum walls inside the cavity, in which case a low loss material with respect to the microwave frequency

such as quartz must be used for the vacuum walls. This approach is used in the matrix isolation system described later.

3.3 MODIFICATIONS TO THE SINGLE CRYSTAL SYSTEM

In the single crystal system the cavity walls are slotted to allow the 100KHz modulation field into the cavity. The cavity walls are much thicker than the skin depth at 100 kHz. The slots are radial to minimise the effect on the electric vector of the microwave field, so as not to affect the Q of the cavity unduly. The slots are arranged in three groups around the circumference of the cavity to provide as much structural rigidity as possible. Three sectors are required so that the modulation is not shorted out.

This slotting however does lower the Q of the cavity, which in turn lowers the sensitivity. Therefore, instead of the full length of the cavity walls being slotted, only the top 18mm of the cavity where the crystal was positioned, was slotted. Although this reduced the "active" portion of the cavity, this was not a problem as only small crystals, which fit easily into this zone, are used. The iris coupling screw had to be placed some distance from the iris on the cavity owing to construction difficulties. This meant that for good microwave coupling between the wave-guide and cavity the size and shape of the iris was quite sensitive.

The optimum iris dimensions were found by trial and error. A photograph of this cavity is shown in fig 3.5.

The materials used in the construction of the cavity and the section of the apparatus around the cavity must be totally non-magnetic so as not to upset the homogeneity of the static field of the spectrometer. Obtaining such materials in New Zealand posed problems especially in the case of stainless steel, with the non-magnetic grade 310 being essentially unobtainable. Heat treatment of work magnetised stainless steel was found to be unsuccessful. A furnace which could be heated to 1000^{o}C with an inert atmosphere was not available. Consequently the stainless steel oxidised badly during the annealing process. As well as this the annealing did not remove all the magnetism from the stainless steel. The cavity was therefore constructed from brass which in New Zealand can contain appreciable amounts of iron. The baseline of this cavity shows a very broad resonance centred about 0.25 T which we believe is caused by impurities in the brass. Phosphor bronze has a much lower iron content and we intended to machine the cavity from this material. However, it is difficult to machine and would probably have degraded our Q significantly as it is not as good a conductor as brass.

The initial design of the cavity system used in this apparatus allowed the cavity to be cooled to near 77 K by passing liquid nitrogen through a labyrinth in the cavity

Fig 3.5 Photograph of the single crystal apparatus cavity assembly.

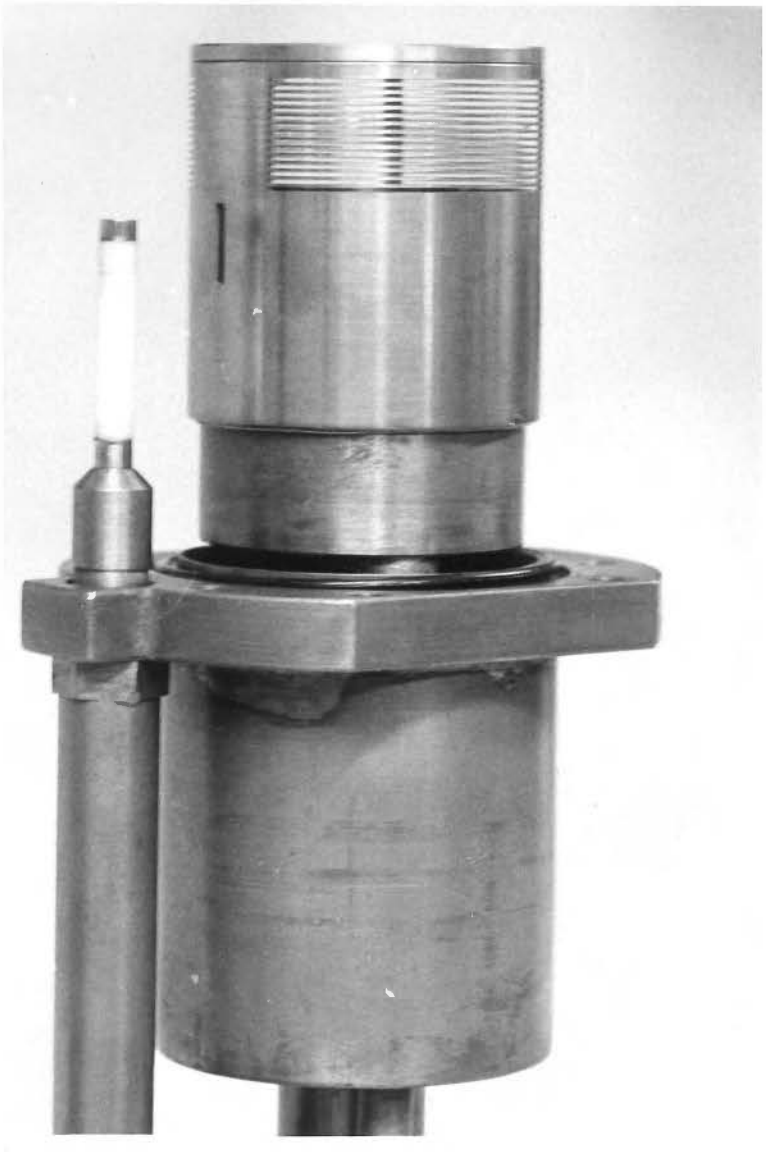

mount. This was to prevent radiative heating of the sample by the cavity although this was found to be unnecessary. The liquid nitrogen entered the cavity mount via stainless steel tubes. These tubes were found to be magnetic and exhibited a very detrimental effect upon the instrumental linewidth and were removed. During the removal process a small piece of one of these tubes, about 5 mm long, became lodged inside the cooling labyrinth and as removing it would have required complete rebuilding of this section of the apparatus, experiments were conducted to assess its effect. The instrumental linewidth was increased to about 0.03 mT, which was clearly unsatisfactory and this piece was removed.

The Air Products Displex model CS202, which cools the sample, uses a pulse expansion of high pressure helium. This causes a low frequency (2.3 Hz) vibration of the sample, which in turn, causes the resonant frequency of the cavity to cycle. This frequency cycling pulls the klystron frequency with it because of the automatic frequency control which locks the klystron to the cavity and as a result of this a modulation is placed on the ESR spectrum. A notch filter [PER75] was installed in the recorder amplifier to remove this modulation.

During the collection of the ESR spectrum the microwave frequency is read by the computer 100 times at the beginning and end of each scan to average out the oscillation in the frequency. (this operation takes about 20 seconds) The NMR

frequency field markers are also read by the computer during a scan and the slope between adjacent markers is calculated. This giving a measure of the accuracy of the markers. As well as this each marker is read three times and a good marker will have all three readings in close agreement. This programme was written using a Pascal main programme which performs the output of the microwave and NMR frequencies and the plotter position to a printer. A series of machine language subroutines communicate with the frequency counter and the ESR spectrometer plotter. The programme was run on an SBC100 system which had had extensive input/output hardware and control logic added to the basic system in order to control and communicate with the spectrometer and frequency counter [BAK85].

3.4 RESULTS OF THE SINGLE CRYSTAL STUDIES

The ESR spectrum of a Ge-doped quartz crystal which had been irradiated by a ^{60}Co source (total dose of 1 Mrad.) was aligned in the apparatus such that one of the a axes was perpendicular to the static field of the spectrometer. This crystal was then rotated about this axis and the ESR spectrum recorded at 10^{o} intervals, the angle being referenced to the c axis of the crystal. Each scan had magnetic field markers placed upon it and the microwave frequency was measured. The computer programme discussed above was used.

The positions of the lines of the A centre were calculated and a least squares fitting programme C111MIN obtained from J. A. Weil was used to optimise the g and A tensors of this centre. The g terms were fitted to $\pm$ 0.0001 and the A terms to $\pm$0.001 mT. The mean difference between the calculated line positions for this centre using the values in Table 3.1 and the experimental line positions was 0.002 mT.

This rotation of the Ge-doped quartz crystal at 12K produced the g and A tensors for the A centre shown in Table 3.1. Also listed in this table is unpublished data for the same centre at a similar temperature obtained by Claridge [CLA76] using the single crystal apparatus of Weil [PER75]. The data obtained in this work and that of Claridge for the A centre is clearly in good agreement.

The sensitivity and operation of this ESR system had been shown to be satisfactory. Nevertheless, the base pressure obtainable was only 2×10^{-5} Torr due to the plastic (Delrin) block which formed part of the cavity system. As well as introducing out- gassing problems this block was shown to be porous. This section of the apparatus was replaced with a brass block containing thin stainless steel (347) foil inserts for the modulation to pass through.

At this time stainless steel foil was commercially unavailable in New Zealand. Three samples of foil alloys 302, 304 and 347 were obtained from Air New Zealand aircraft

Table 3.1

Principal magnetic parameters of the A centre in irradiated Ge-doped quartz at 12K

this work				Claridge & Weil			
g ±0.0001	θ (degrees)	A ±0.001 mT	θ (degrees)	g ±0.0001	θ (degrees)	A (mT) ±0.001	θ (degrees)
2.0018(5)	66.7	-0.038(4)	26.1	2.0017(6)	66.8	-0.042	28.7
2.0001(9)	90.0	-0.044	116.1	2.0000(8)	90.0	-0.048(2)	118.8
1.9911(2)	23.3	-0.102(4)	90.0	1.9908(6)	23.2	-0.105(9)	90.0

Calculated at a constant field of 0.332 T

Calculated at a constant field of 0.352 T

maintenance department. The 347 alloy which was used was the least magnetic and was not annealed before use.

Unfortunately the brass block was unsatisfactory as there was insufficient modulation at the sample available and the stainless steel inserts were too magnetic for reasonable line-widths.

CHAPTER IV

MATRIX ISOLATION ESR APPARATUS

The cavity arrangement of the single crystal system was found to be unsatisfactory for the matrix isolation due to its high leak rate. This system was not constructed for high vacuum but only intended to function below 10^{-4} Torr where conduction heating of the sample by surrounding gas would be negligible. The single crystal cavity system was replaced with a standard Varian E-235 cylindrical cavity. The top plate of the E-235 cavity was replaced with an aluminium adapting plate into which a silica tube was sealed with an O-ring. Photographs of this assembly are given in fig 4.1. The sample fitted into the cavity inside the silica tube. In this way all parts of the vacuum system were made of vacuum compatible materials and when it was found that insufficient pumping speed could be achieved by pumping from just the back port, an extra 2" oil diffusion pump was attached to the silica tube via a double surface glass liquid nitrogen cold trap. This trap was later replaced with a single surface stainless steel version after two glass types imploded. Also the rate of boil-off of the liquid nitrogen from the glass cold-traps was unacceptably high. The stainless steel cold trap was helium leak tested using a quadrupole mass spectrometer. Using two diffusion pumps the base pressure was typically 7×10^{-7} Torr.

Fig 4.1 Upper. Aluminium adapting plate and quartz tube. Lower. Adapting plate and tube installed in Varian E-235 cavity.

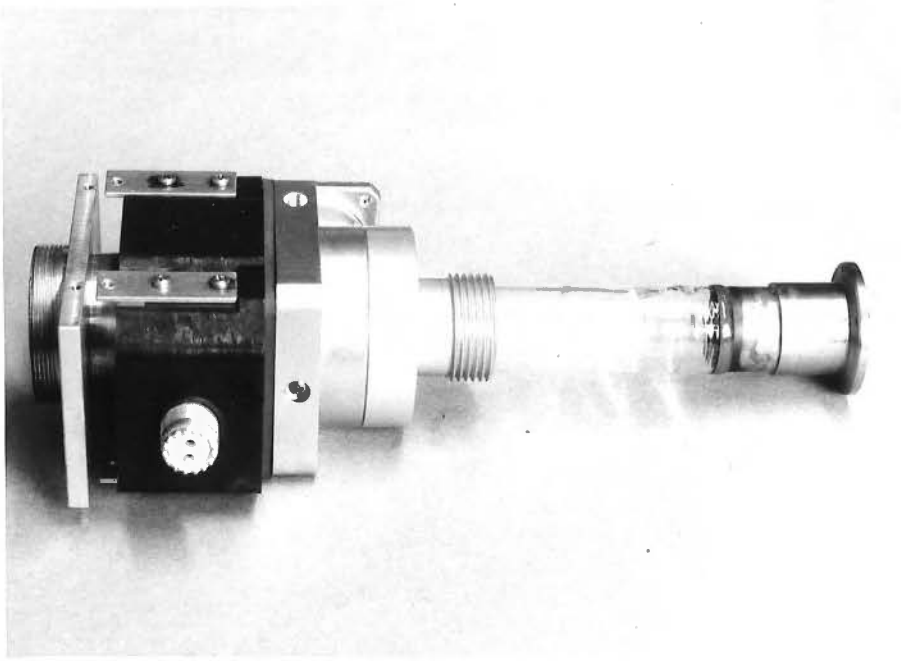

The matrix support was an 18 mm diameter copper rod machined down to 3 mm diameter at one end. This rod was screwed into the base of the Displex expander unit and could be raised 75 mm to a position where deposition of the matrix occurred. At this position an 18 mm port and a stainless steel capillary were aimed at the same point on the support. The matrix gas was injected through the capillary and the ion source attached to the vacuum port. After a period of deposition the support could be lowered into the cavity to record the ESR spectrum of the matrix.

The vacuum system for the ion source was the same as for the gas phase studies (fig 2.4 P 32) except that the silica tube was replaced with a short length of 18 mm O.D. pyrex tube. This tube was sealed into the 18 mm port of the matrix isolation system with an O-ring. Only minimal shielding was required for the ion source as the magnet was not on during deposition

4.1 MATRIX ISOLATION EXPERIMENTS WITH ION SOURCES

Initially experiments were conducted to determine the ion current available at the matrix support.

The ion current at the matrix support was measured at room temperature by replacing the Displex assembly with a 3mm brass rod attached to a vacuum electrical feed-through. The typical ion current measured was 150 nA and as described

earlier optimum currents were found when the ion source was operated at as low a pressure as possible. When argon matrix gas was added through the capillary bringing the total pressure up to 4 x 10^{-5} Torr the ion currents measured dropped 30% . Assuming an ion current of 100 nA, 10^{12} ions per second are arriving at the matrix support. If deposition is continued for two hours and if the trapping efficiency is 1% or greater, trapped ions should be observable.

In a typical experiment after the Displex had cooled down to around 10K the ion source was started. The source pressure was then minimised, the pressure at the cavity measured and argon matrix gas added to bring the total pressure up to between 2 and 8 x 10^{-5} Torr. This corresponded to at least a twenty fold excess of matrix gas measured as a function of the relative pressures of uncondensed material.

4.2 RESULTS

Using argon through the ion source and argon matrix gas, the background level of impurities was determined. Nitrogen and hydrogen atoms and methyl radicals were observed. With the source off but an ion gauge unit operating during deposition 7cm away from the matrix support, a similar spectrum was produced. This apparatus then was very sensitive to neutral radicals formed from impurities in the

argon or the general background in the vacuum system. NZIG welding grade argon, the highest purity available locally, was used.

In order to purify the argon it was passed through a mixture of magnesium and sodium metals in a furnace at 550 ^{o}C and then through 4A molecular sieves at -78 ^{o}C. At first a silica tube was used to contain the magnesium sodium metal mixture in the furnace but the inside surface of this tube was found to crack badly probably as a result of alkali corrosion. Later a heavy walled stainless steel tube (316) was used in the furnace. This purification significantly reduced the level of nitrogen and hydrogen atoms. Matheson UHP argon was obtained and this offered some further improvement.

The diffusion pump oil that was used was a silicone oil and therefore a likely source of methyl radicals. This oil was replaced with a poly-phenol based oil, Sanovac 5 (Monsanto). These steps reduced the methyl radical concentration but it was still high, probably due to out-gassing from the O-rings and associated vacuum grease used in the apparatus.

In this series of experiments, no evidence of ions trapped in the argon matrix was observed.

Carbon monoxide as a source gas produced the usual

background and the HCO radical [COC66].

Ammonia produced NH_2 radicals [COC69] and a high level of hydrogen and nitrogen atoms.

Methane produced a large increase in the methyl radical signal.

2-methyl-pentene, cyclo-hexene and benzene produced the normal background as well as C_2H [COC64] radicals and a singlet at slightly lower g value than nitrogen atoms. In the experiments using benzene, a small signal consisting of a large number of lines could be seen and this signal was probably phenyl radicals. The signal intensity was too small to permit analysis as it did not seem to be isotropic. In one experiment benzene was added to an argon ion beam. The C_2H signal was more pronounced and the singlet was absent.

It was not possible to assign the singlet at $g = 2.0013$ (measured relative to the nitrogen atom signal using a value of 2.0017 [KNI82] which is the g value of nitrogen atoms in neon) observed when cyclo-hexene 2-methyl-pentene or benzene are passed through the ion source. However it seems likely the radical responsible for this signal is a small molecule as it is only formed under the harsh conditions of the ion source.

The failure to observe ions trapped in argon in these experiments was ascribed to the high energy of the ions. Most of the beam would have an energy above 2 keV, which would lead to fragmentation and charge transfer reactions with the matrix gas. As well as this the ion beam contains some electrons which would move rapidly through the matrix, neutralising some of the positive ions.

4.3 TEMPERATURE CONTROL AND MEASUREMENT

The hydrogen atoms observed in these experiments were found to be trapped in three sites. Annealing the matrix produced one site. At this stage, we were unable to monitor the temperature of the matrix support accurately, and as temperature effects had been observed it was decided this facility was required. The temperature of the matrix support was controlled by an Air Products model 3610 Temperature Controller. The temperature of the base of the second stage of the Displex was determined by either a platinum or germanium resistance thermometer. A particular value for the resistance of the sensor, which corresponds to a particular temperature, was set on the controller. Using a heater, also placed on the second stage of Displex, the temperature of the second stage was controlled at this value. The sensors were uncalibrated so absolute temperature measurement was not possible. It was decided a separate device to measure the temperature would be the simplest approach.

The most convenient way of measuring a temperature in this region is a 0.07% atomic iron/gold versus chromel thermocouple (Oxford Instruments). The sensitivity of the thermocouple is about 0.040 mV K^{-1} and the output at 10 K, with an ice/water reference is about 4.2mV. A suitable D.C. voltmeter was not available so an amplifier was constructed to drive a 200 mV, 3.5 digit LCD digital voltmeter unit. A gain of 37 gave a resolution of $\pm$ 0.15 K. As the thermocouple could only be calibrated before it was installed on the Displex and there after only with great difficulty, it was important that the amplifier had good long term stability. It was constructed using a high quality low drift chopping operational amplifier and low temperature coefficient components. A circuit of the amplifier is given in Appendix III. The amplifier was mounted in a copper box filled with insulating material to minimise the effects of drafts and this was mounted directly on the expander unit of the Displex. The output of the thermocouple has been reported to be affected by magnetic fields [WHI79] if a region of the thermocouple subject to a temperature gradient is also in a magnetic field. No evidence of a magnetic field dependence of the output of the thermocouple with the field strengths and physical lay-out used in these experiments was observed.

The thermocouple junctions and the critical junctions in the amplifier were soldered with low contact potential cadmium solder. Calibration of the thermocouple with ice/water as a reference, was performed at the boiling point

of helium, 4.2K, the boiling point of nitrogen, 77.4 K, the melting point of pentane, 143.5 K, and the sublimation point of CO_2, 194.6 K. The values obtained at these temperatures were fitted to a cubic function.

$$T(K) = A.T(mv)^3 + B.T(mv)^2 + C.T(mv) + D$$

where A = -1.2303(-5) , B = -1.0323(-3) ,
C = -1.3303 , and D= -273.298 .

4.4 EXTRA-NUCLEAR ION SOURCE

Attempts to trap ions in an argon matrix using the CPO ion source had been unsuccessful due to the high energy of the ion beam. Work published by Knight et al. [KNI82] at about this time stated that they had been unable to trap NH_3^+ in an argon matrix. The NH_3^+ was formed at essentially zero energy by photolysis using argon resonance radiation. Knight et al. also mentioned the comments of Bondybey, as discussed in the introduction, about the limitations of argon as a matrix for ions. An Extra-Nuclear ion source was available which would produce reasonable ion fluxes at low energies so it was decided to try this ion source.

The ion source was mounted in a brass cup attached directly to the 18mm vacuum port on the matrix isolation apparatus. Attached to the back of this cup was a stainless

steel capillary to supply the source gas and a 3" brass tube. This was connected to a 2" diffusion pump to pump the area around the ion source. A cross sectional view of the ion source mounting system is shown in fig 4.2. The ion beam current from this ion source was considerably smaller than the CPO source. With an ion energy of 17 eV, ion currents at the deposition target were typically 10 nA. Mixtures of 1:100 ammonia in argon were passed through the ion source at 1×10^{-4} Torr, and deposition was continued for up to five hours. Methyl radicals and nitrogen atoms were observed but there was no evidence of hydrogen atoms or NH_2 radicals or NH_3^+. The ionising conditions and ion energies were not so conducive to fragmentation with this ion source. This explains the lack of a NH_2 signal but the absence of hydrogen atoms whilst nitrogen atoms are being produced by this ion source is puzzling. Our failure to observe NH_3^+ was not surprising as the ion energy was still quite high at 17 eV.

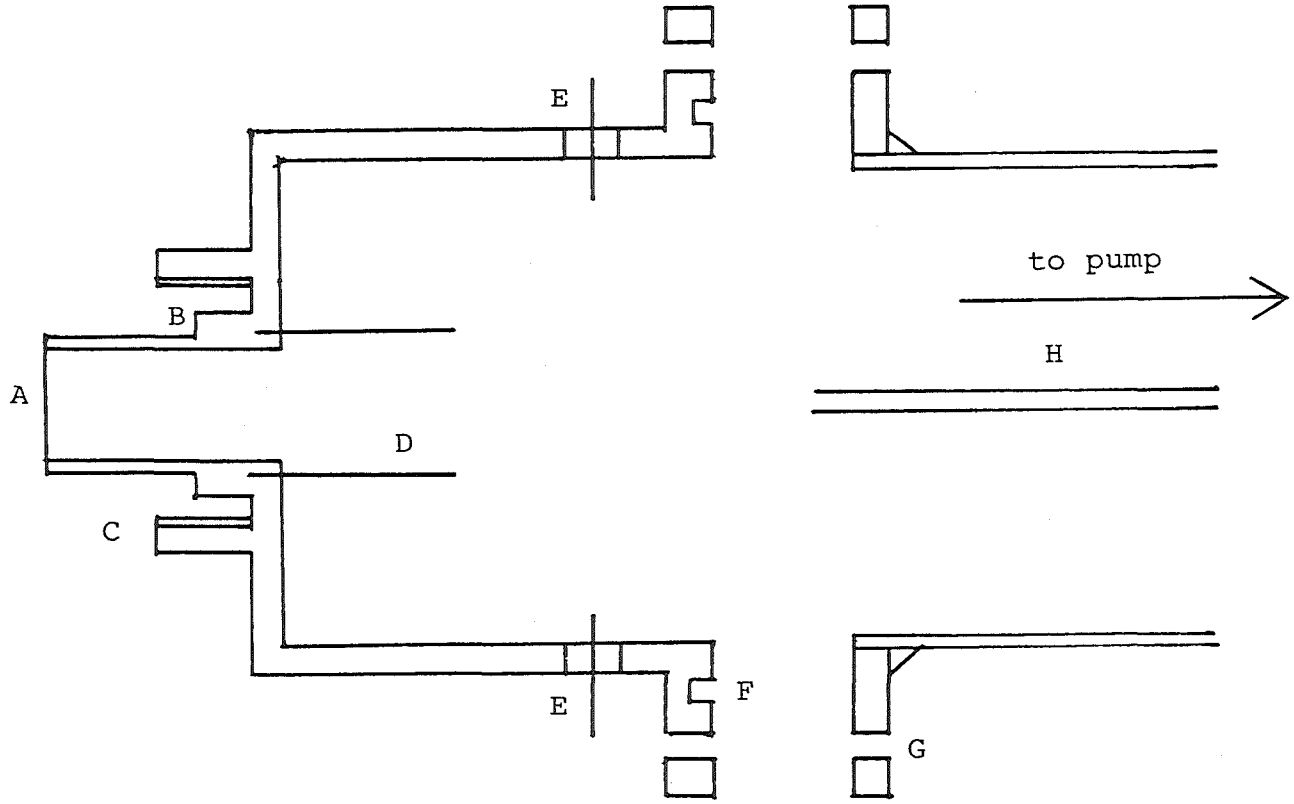

Fig. 4.2 Sectional view of Extra Nuclear ion source mount. A 18 mm spigot, B O-ring, C 30 mm thread screws into thread around vacuum port, D 10 B.A. studs to mount ion source, E Vacuum "lead thrus ", F O-ring groove, G bolt holes, H gas inlet capillary

CHAPTER V

PHOTOLYSIS EXPERIMENTS

Electostatic ion sources had proved unsuitable for generating ions to trap in an argon matrix due to the energy of the ions. It was decided to use vacuum ultra-violet (VUV) photolysis as a source of ions. This technique is well established, although with a few exceptions, argon resonance radiation (11.6, 11.8 eV [OKA78]) is not of high enough energy to ionise small molecules. We intended to repeat the experiments of Knight et al. [KNI82] as ammonia with an ionisation potential of 10.2 eV [ROS77] appeared a likely candidate.

The VUV lamp was connected in line with the 18mm port on the matrix isolation apparatus. The lamp was made in two parts, as shown in fig 5.1. The first part was a small cup containing the window glued in with Torr Seal (Varian). The second part of the lamp was a 15 cm length of silica tube with a needle valve on one end and an outlet leading to a mechanical pump at 90^{o} to the silica tube. A flow of argon at low pressure passed through the lamp and was excited by a microwave discharge (Raytheon 125W diathermy unit). The discharge must touch the window to minimise resonance absorption. A LiF window was used for most experiments. The window tends to absorb some of the radiation thus forming colour centres degrading its transparency. Regular annealing

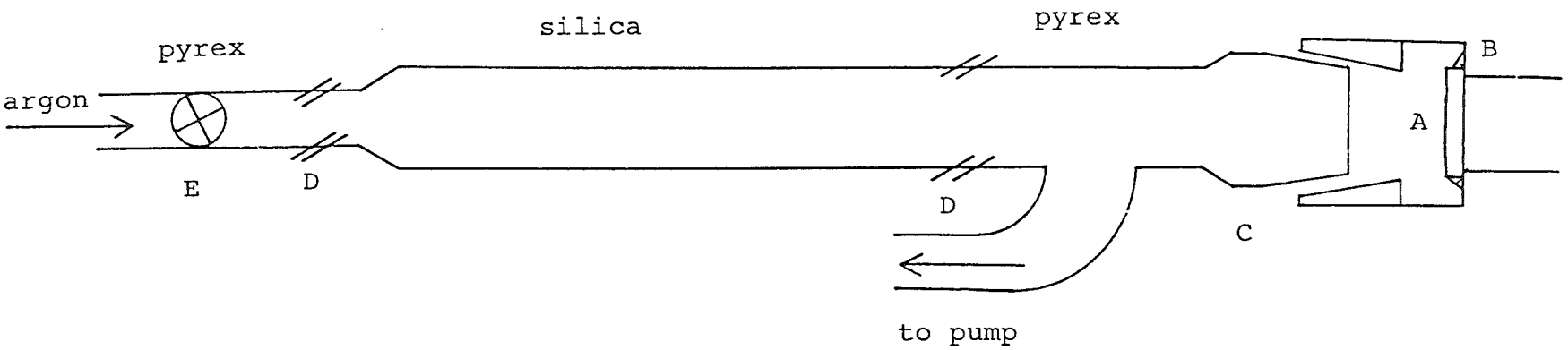

Fig. 5.1 Diagram of flowing vacuum ultra violet discharge lamp. A VUV window, B Torrseal (Varian), C B34 tapered joint, D silica to pyrex graded seal, E teflon/ pyrex needle valve.

of the window at 450 ^{o}C restored its transparency. The Torr Seal also degraded under exposure to the VUV radiation and the windows had to be replaced about every six hours of operation.

Constructing the lamp in two parts also allowed photolysis using either a mercury resonance lamp or a high pressure mercury lamp, without bringing the matrix isolation apparatus up to atmosphere. In this way, radicals could be generated using VUV radiation and the effect of lower energy photolysis could be studied.

Gas mixtures of the matrix gas, usually argon and the species to be ionised, were prepared in a glass handling line using a Baratron capacitance manometer (MKS) and a mercury manometer to determine the ratio. The glass handling line was pumped by a 2" diffusion pump. The pump was equipped with a liquid nitrogen trap and used Sanovac 5 (Monsanto) pump oil. Typical base pressures of 2 x 10^{-7} Torr were obtained. The gas mixture was then injected into the matrix isolation apparatus to be coincident with the VUV photolysis. The background pressure increased to between 2 and 8 x 10^{-5} Torr during deposition. This corresponded to a flow rate of around 5 mMol h^{-1} . Deposition was usually continued for two hours.

5.1 INITIAL RESULTS

Ammonia mixtures in argon ranging from 50 to 200 ppm were found to give rise to an ESR spectrum when irradiated with argon resonance radiation (11.4,11.6 eV [OKA78]) which did not correspond to the NH_2 radical spectrum observed under the same conditions when mercury resonance radiation (6.7 eV [OKA78]) was used. Parts of the spectrum were largely masked by methyl radical and nitrogen atom signals. A blank experiment with argon only showed the usual background of nitrogen, hydrogen atoms and methyl radicals. Deuterated ammonia, ND_3, was synthesised by the addition of D_2O to Mg_3N_2. The Mg_3N_2 was prepared by passing nitrogen gas through a silica tube containing magnesium metal at 550^oC. Photolysis during deposition of a mixture of ND_3 and argon gave the same spectrum as obtained with NH_3 but with the addition of a deuterium atom signal. The deuterium atom signal was still present even after several months and many cycles of exposure of all the parts of the apparatus to atmosphere.

The form of the spectrum observed with the argon resonance photolysis of ammonia argon mixtures, a quartet of triplets (fig 6.1, P 86), suggested NH_3^+ to be the radical trapped. This assignment was, however, suspect because of the negative experiment with ND_3, and the anisotropic nature of the spectrum. Whereas NH_3^+ trapped in a neon matrix is isotropic [KNI82]. At this time a

programme to simulate powder-type spectra was not available.

The concentration of impurities in the matrix was obviously high. The signal level of each impurity exceeded that of the NH_3^+ signal. Therefore it was decided to completely redesign and rebuild the matrix isolation apparatus in an effort to eliminate the possibility the observed spectrum was caused by impurities in the matrix. At the same time the possibility of obtaining and using $^{15}NH_3$ and obtaining a programme to simulate powder spectra was investigated.

5.2 FINAL DEVELOPMENT OF THE MATRIX ISOLATION APPARATUS

The apparatus described in Chapter III and IV had ten O- rings close to the deposition target. Two of these O-rings had to be well greased as they provided a moving vacuum seal allowing the Displex assembly to be moved up for the deposition of the matrix. The objective in the new design was to eliminate as many O- rings as possible especially those which required to be greased.

Movement of the Displex was achieved using a stainless steel bellows. Due to constraints imposed by the bellows the movement of the matrix support between the cavity and the deposition position was reduced to 50 mm. In order to maximise pumping speed to the area where deposition occurred the largest possible area of pumping tube was used. This

entailed using two 50 mm square stainless steel tubes joined side by side. A turbo-molecular pump (Sargent Welsh model 3113C) with a pumping speed of 1100 l s^{-1} replaced the oil diffusion pumps. The windows were sealed to the apparatus using an O- ring in order to simplify as much as possible the process of changing them. The apparatus was thoroughly cleaned with chlorinated solvents to eliminate any source of methyl radicals from the metal surfaces. Finally, the apparatus was designed to be partially bakeable. A diagram of this apparatus is shown in fig 5.2 and photographs of the complete experimental apparatus appear in figs 5.3 and 5.4.

The apparatus was helium leak tested using a quadrupole mass spectrometer (Spectramass). A base pressure of 2×10^{-8} Torr was attained. The methyl radical signal was considerably reduced but the hydrogen atom signal was still quite high. The residual level of the contaminants was probably due to impurities in the argon (Matheson UHP). A new signal appeared in the background spectrum using this apparatus, a closely spaced doublet (U on fig 6.1, P 86) at $g = 2.0282$ and with a spacing of 0.044 mT. As the signal was not present in the earlier apparatus it is likely this signal is caused by a decomposition product of the trichloroethylene used for cleaning or from some residual of the flux used during welding of the vacuum system. The silver soldering used a fluoride based flux and the soft soldering flux was phosphoric acid.

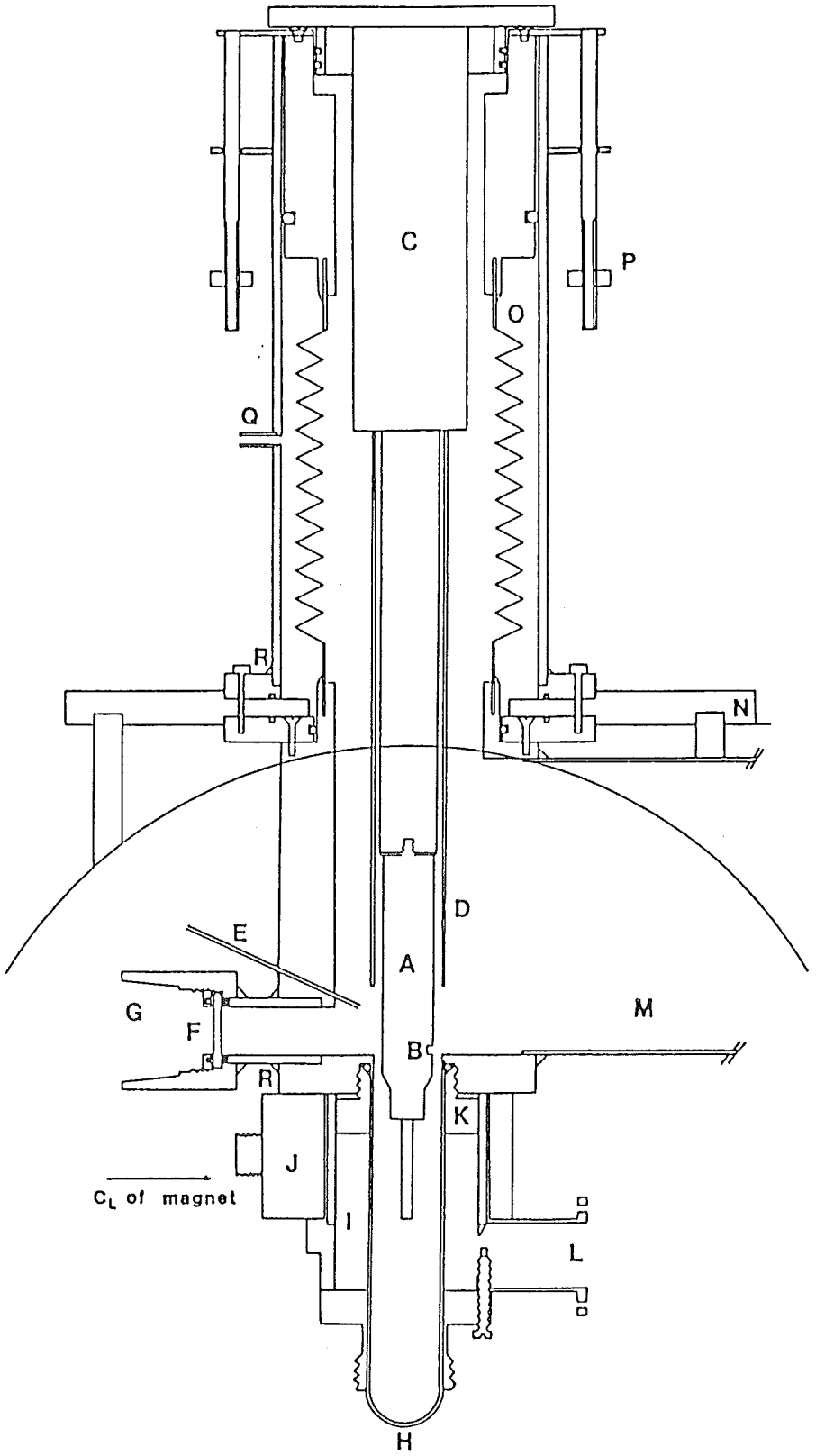

Fig. 5.2 Diagram of final matrix isolation ESR apparatus. A matrix support, B position of thermocouple, C Displex, D second stage heat shield of Displex, E matrix gas injector, F VUV window, G VUV lamp attachment, H 25 mm silica tube, I Varian E-235 cylindrical cavity, J cavity modulation coils, K cavity adapting plate, L microwave wave-guide, M pumping port, N supporting plate, O stainless steel bellows, P limit movement when Displex raised for deposition, Q compressed air inlet to raise Displex. All joints are silver soldered except those marked R which are soft soldered.

Fig 5.3 Photograph of matrix isolation apparatus from the front of the spectrometer magnets.

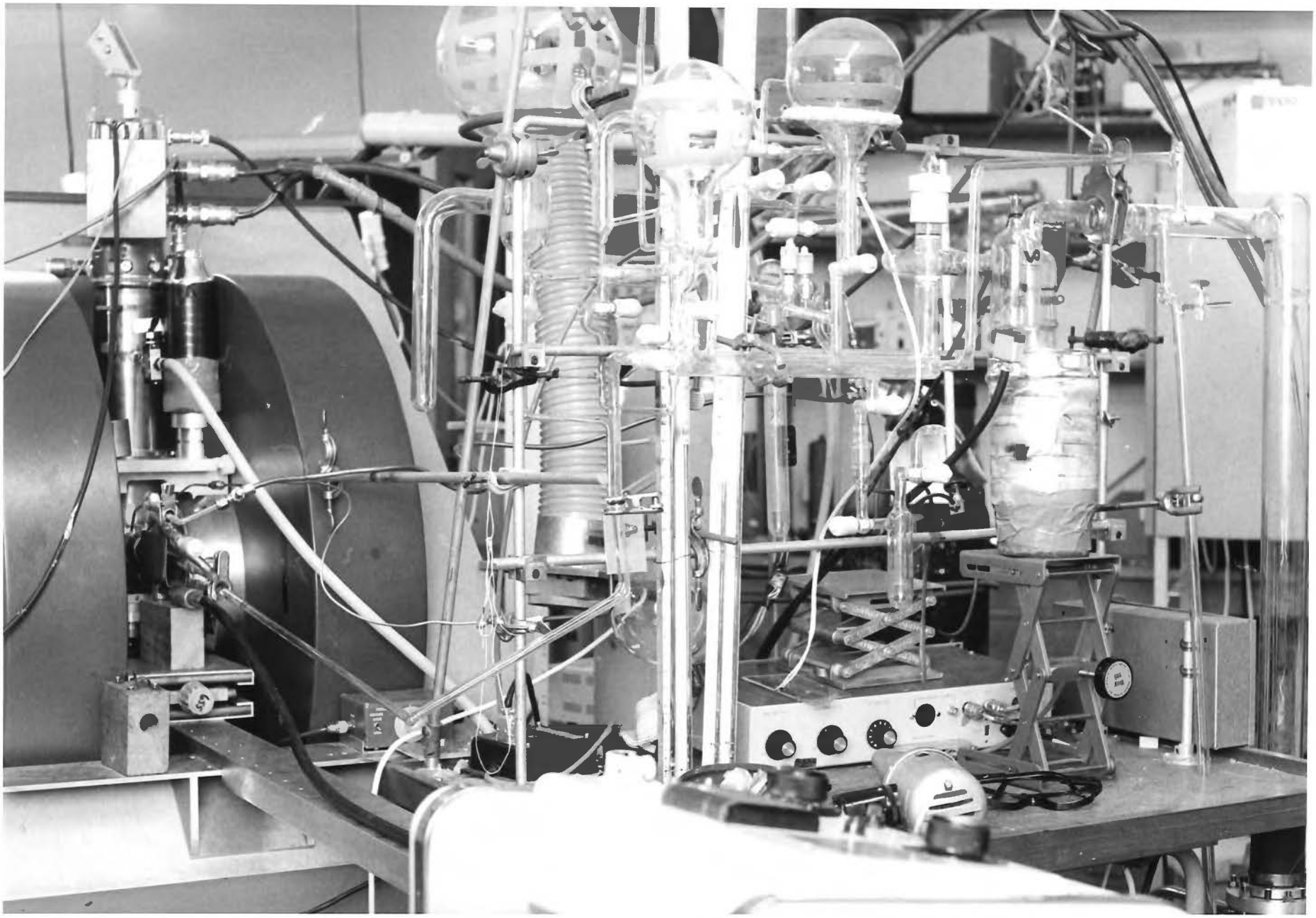

Fig 5.4 Photograph of matrix isolation apparatus from the rear of the spectrometer magnets.

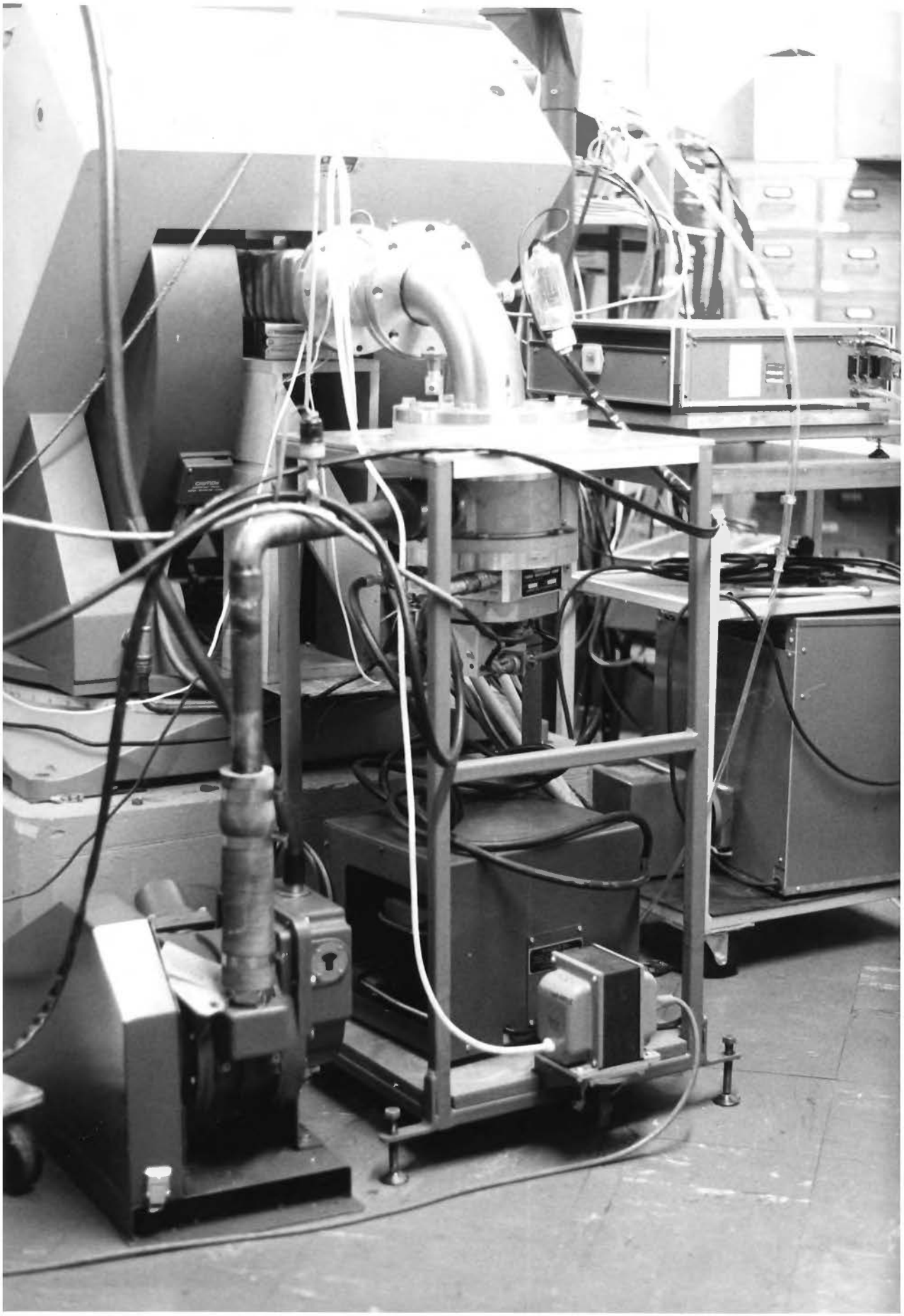

The new apparatus gave a background in which the signal of each contaminant was less intense than the major NH_3^+ lines.

$^{15}NH_3$ was prepared by the reduction, under a reduced pressure of air, of $Na^{15}NO_2$(Merck Sharpe and Dohme) with Devarda's alloy and KOH [SPI62]. Experiments in which $^{15}NH_3$ argon mixtures were photolysed with argon resonance radiation during deposition confirmed the species formed as NH_3^+.

As an indication of the elaspsed time in some of the construction phases of this project the original drawings for this new apparatus were submitted in February 1984 and the apparatus was not completed until January 1985. There-after all proceeded well until a main bearing failed on the turbo-molecular pump during April 1985, see fig 5.5. Unfortunately there was little warning of this failure and the results were rather final.

Fig 5.5 Photograph of the turbo-molecular pump after one of the main bearings collapsed during operation.

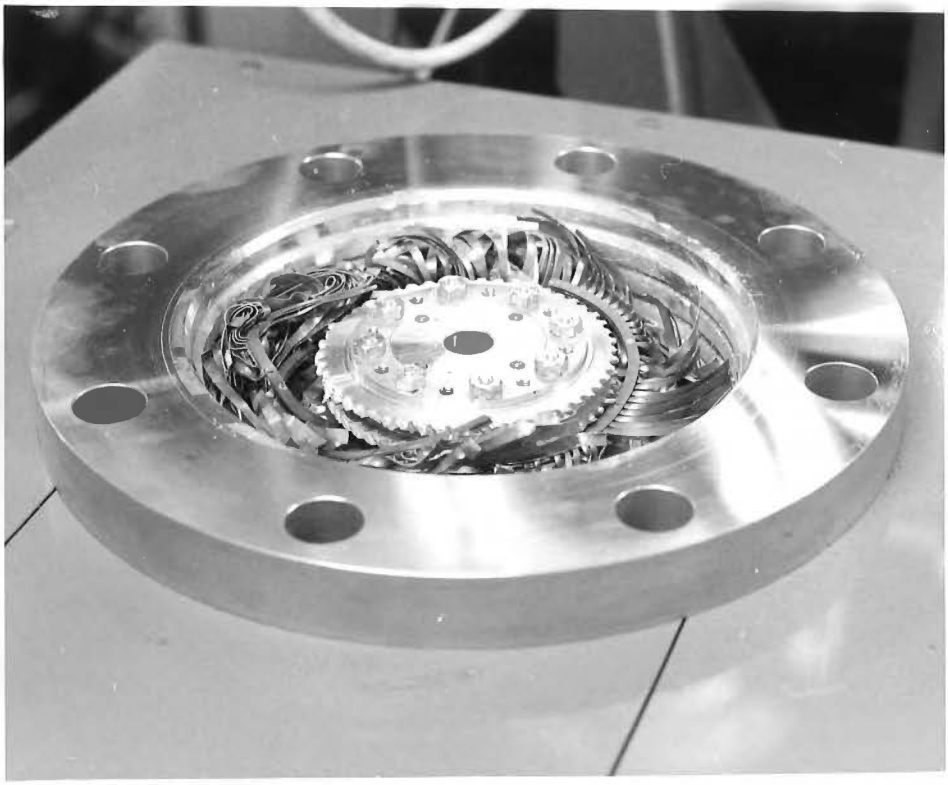

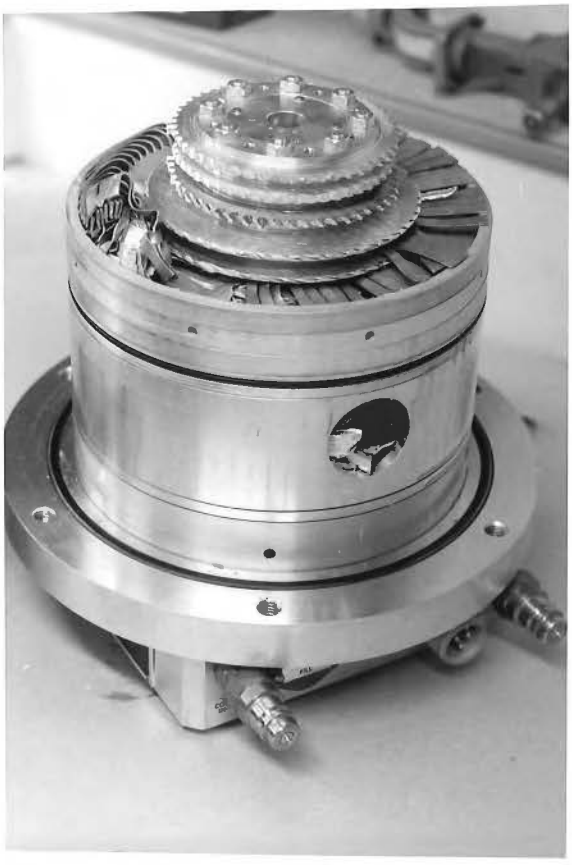

CHAPTER VI

RESULTS OF PHOTOLYSIS EXPERIMENTS

The results of all experiments using vacuum ultra violet photolysis will be discussed in this section. In all cases a general background of methyl radicals, and hydrogen and nitrogen atoms was observed. All g values quoted were calculated relative to another known species in the matrix. In most cases, except where specifically mentioned, g values were determined relative to the g value of nitrogen atoms. The g value of nitrogen atoms in argon has not been measured accurately but a value 2.0017 [KNI82] is available for neon matrices and since a significant matrix shift is unlikely this value was used. Computer simulations of powder spectra were performed on the Prime 750 mini-computer and outputted onto the Hewlett Packard plotter of the University of Canterbury central computing facility. The simulation programme used was written by P. H. Kasai and obtained from L. B. Knight. Only slight modifications in the graphic output subroutine were required for the programme to be executed on the Prime.

A powder ESR spectrum results from the radicals which are trapped in random orientations with respect to the spectrometer field. Consideration of the theory [WER72] shows the ESR spectrum observed in this case will be a sum of the spectra of the individual radicals trapped in the matrix.

The observed spectrum may be calculated by integrating the spectrum of a single radical over all orientations. The simulation programme used in this work produces powder spectra by this summation method.

6.1 AMMONIA EXPERIMENTS

The ESR spectrum observed from a matrix at 14K formed during argon resonance photolysis (11.6, 11.8 eV) [OKA78] of an ammonia argon mixture is shown in fig 6.1a. The spectrum is largely masked by signals resulting from impurities and other products of the photolysis; CH_3 radicals (M), nitrogen atoms (N), NH_2 radicals (A) and an unknown radical (U). Examination of the remaining spectrum, shows it to be composed of a quartet of triplets, having an anomalous intensity ratio and lineshape resulting from individual NH_3^+ radicals trapped in fixed orientations within the matrix. This results in an ESR spectrum which is an average over all orientations. A computer simulation of the spectrum observed for $^{14}NH_3^+$ using the parameters in Table 6.1 is shown in fig 6.1b. The same experiment performed with $^{15}NH_3$ produced the expected spectrum consisting of a quartet of doublets shown in fig 6.2a. A simulation, fig 6.2b using the parameters for $^{14}NH_3^+$ and using a ratio for $A(^{15}N)$ to $A(^{14}N)$ of 1.403 [WER72] is in good accord with the observed spectrum. Refinement of the parameters for the hydrogen atoms and the g factor could possibly improve the fit. An identical experiment using a Hg resonance lamp

(6.71 eV) [OKA78] produced only the expected NH_2 radical [COC69] spectrum and the usual contaminants. There was no evidence of the NH_3^+ signal.

Replacement of the argon resonance lamp with a static krypton lamp (10.03, 10.64 eV) [OKA78] and a LiF window produced the same spectrum. When the window was changed to MgF_2, acting as a cut-off filter attenuating the higher energy resonance line of krypton at 10.64eV, leaving the 10.03eV line, the observed NH_3^+ spectrum was significantly decreased in intensity. In a further experiment the window of the argon resonance lamp was replaced with a brass disk which had a 0.5mm hole drilled in the centre. An identical spectrum of NH_3^+ trapped in argon was observed. Addition of an electron scavenger, SF_6, at equal concentration to the NH_3 in argon, typically 100ppm, did not appear to increase the yield of trapped NH_3^+ significantly. Attempts to form NH_3^+ trapped in a krypton matrix using photolysis from an argon resonance lamp and a LiF window proved unsuccessful.

Following the formation of the NH_3^+, radical cation, trapped in the argon matrix, photolysis of the matrix with a 200W Hg lamp, filtered with a silica cell filled with water to remove infra red radiation, produced no observable change in either the intensity or positions of the NH_3^+ lines. Photolysis was continued for up to thirty minutes. Substitution of either ND_3 or NH_2D for the NH_3 produced

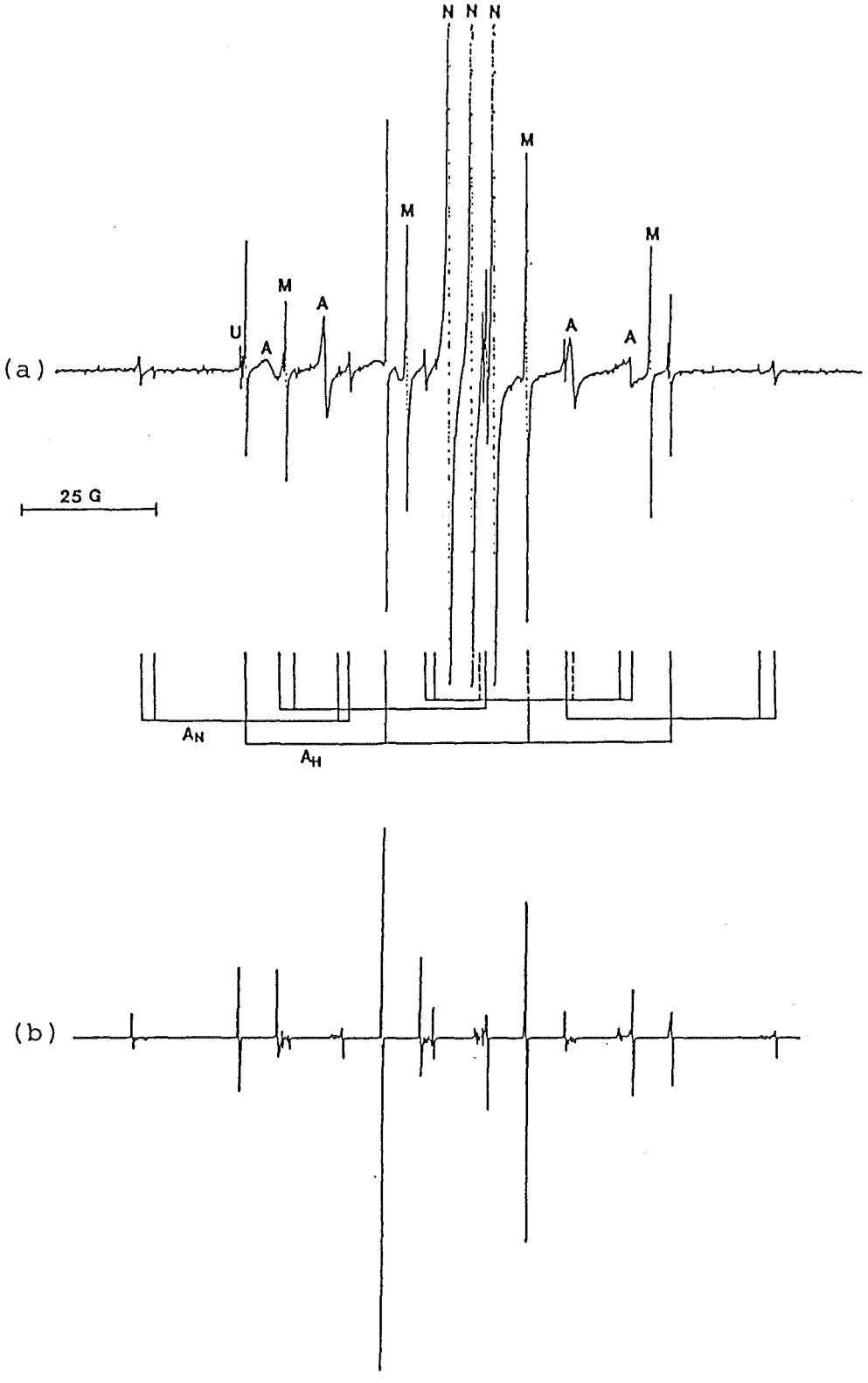

Fig. 6.1 (a) ESR spectrum of NH_3^+ trapped in an argon matrix at 12 K. M methyl radicals, N nitrogen atoms, U unknown radical. (b) computer simulation.

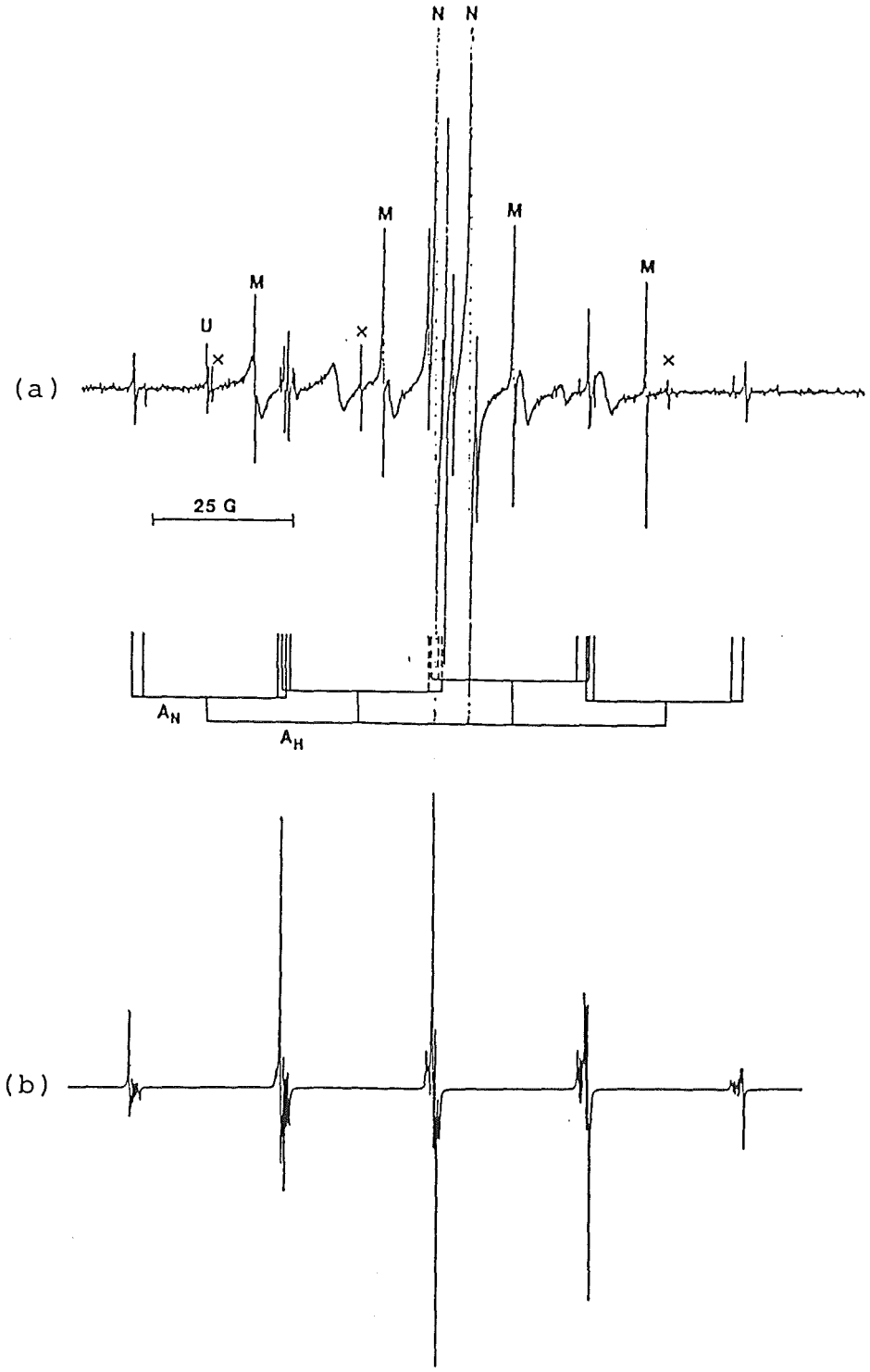

Fig. 6.2 (a) ESR spectrum of $^{15}NH_3^+$ trapped in an argon matrix at 12 K. M methyl radicals, N nitrogen atoms, U unknown radical, x residual $^{14}NH_3^+$ lines. (b) computer simulation.

Table 6.1 The magnetic parameters of NH_3^+ (MHz)

	g_{iso}	$g_{//}$	$g_{\perp}$	A^N_{iso}	A^H_{iso}	$A^N_{//}$	$A^N_{\perp}$	$A^H_{//}$	$A^H_{\perp}$
trapped in argon at 12K. (this work)	2.0033	2.0034	2.0033	52.5	74.2	52.8	47.9	75.0	74.2
trapped in neon at 4K. [KNI82]	2.0032			54.9	76.8				
Single crystal NH_4ClO_4(300 K) [COL61]	2.0035	2.0039[a] 2.0038	2.0032	54.6	72.5	61.8[a] 53.3	48.7	72.3[a] 73.5	71.6
Powdered NH_4ClO_4 (373 K) [HYD61]	2.0034			51	70				

[a]the NH_3^+ was not axial

no new lines in the spectrum observed from the matrix, with the exception of deuterium atom signals.

In all the above experiments the ionising photolysis occurred concurrently with the deposition of the matrix. Photolysis of an existing NH_3/Ar matrix, using the argon resonance lamp and a LiF window, produced little NH_3^+. However, if a krypton resonance lamp was used, reasonable yields could be obtained. This is probably due to the opacity of the argon matrix to its resonance radiation.

When an argon matrix containing NH_3^+ was warmed up the linewidth of the NH_3^+ signal increased with temperature, consequently decreasing the intensity of the lines. The linewidth of the NH_3^+ signal did not decrease again as the temperature of the matrix was raised prior to matrix sublimation when all signals were lost. The effect of the temperature on the $M_I^N=0$: $M_I^H=-3/2$ line, the most intense line of the NH_3^+ spectrum was an increase of the linewidth from 0.01mT at 12K to 0.04mT at 27K.

6.2 DISCUSSION OF AMMONIA EXPERIMENTS

The solution obtained by computer simulation of the spectrum of the radical, observed trapped in argon, shows three equivalent hydrogen atoms and one nitrogen atom. The use of $^{15}NH_3$ confirms the presence of only one nitrogen atom in the radical. The photo-bleaching effect, whereby

exposure of a rare gas matrix to visible light causes a reduction of the trapped cation signal, was not observed. This effect is considered [AND79] to result from photo-detachment of electrons from weakly bound negative ions trapped within the matrix. These electrons then move rapidly through the matrix, neutralising the trapped cations. This effect relies on the transparency of the matrix to visible light. In our experiments the deposition rate of the matrix was relatively slow, 5 mMol h^{-1} compared with 24 mMol h^{-1} used by Knight et al. [KNI82], although these figures are arbitrary since they refer to the gas flow directed towards the matrix support, not necessarily the flow actually trapped. This low deposition rate could have caused a more poly-crystalline matrix in our case which would be more opaque to visible light. However, it is also probable that a low dissociative attachment cross-section for NH_3 precludes the formation of a significant negative ion population in the matrix. Negative ion formation in the gas phase is a resonance process and only a small fraction of the electrons liberated in the photoionisation of NH_3 would have sufficient energy to undergo resonance capture. As a significant matrix shift in the ionisation potential of NH_3 was not observed, in the krypton resonance lamp experiments, ionisation either occurred in the gas phase or the electron acceptor in the matrix was not strong and not close to the resultant NH_3^+ ion.

The experiments using the krypton lamp show the energy

required for the formation of the radical lies between 10.03eV and 10.64eV which corresponds well with the ionisation potential of NH_3 (10.19eV) [ROS77] . The magnetic parameters obtained from the radical shown in Table 6.1 are in remarkable agreement to those of NH_3^+ trapped in a neon [KNI82] matrix and NH_4ClO_4 [COL61, HYD61] crystals confirm the identity of the radical under observation as NH_3^+.

Unsuccessful attempts to trap NH_3^+ in an argon matrix have been reported previously [KNI82]. The signal levels observed in the experiments of this project are very low compared with those of NH_3^+ trapped in neon as observed by Knight et al.[KNI83a]. The spectrometer configuration used in this work should allow a detection limit significantly lower than the rectangular cavity which was used in Knight's work. The failure to observe NH_3^+ trapped in argon has been ascribed to the small difference in ionisation potential between the host matrix and the guest molecule. Failure to detect NH_3^+ trapped in krypton in this study is consistent with this argument. NH_3^+ has one of the highest ionisation potential of any cation trapped in argon whereas krypton has a lower ionisation potential than argon.

The failure to observe the trapping of deuterated derivatives of NH_3^+ in an argon matrix is probably due to rapid deuterium hydrogen exchange reactions during the

deposition process. Even after attempts were made to saturate the vacuum system and gas handling line with ND_3 the hydrogen atom signal was more than ten times higher than the deuterium atom signal. In all experiments using ND_3 and NH_2D, NH_3^+ signals could be observed.

The effect of temperature upon the NH_3^+ signal is a sudden but reversible broadening of the lines. A similar effect has been observed by Knight et al. [KNI83b] for H_2O^+ trapped in neon. Knight observed large differences in the ratio of the intensities of individual hydrogen hyperfine lines between various neon matrices and a partial preferential orientation of the H_2O^+ within the neon matrix. While we did not observe gross differences in the NH_3^+ spectrum from matrix to matrix the possibility of a preferential orientation effect was not fully tested as rotation of the matrix support with respect to the static spectrometer field was not possible with this apparatus. The strong temperature effect upon the linewidth could perhaps suggest some kind of preferred orientation of the NH_3^+ molecules within the matrix. Slight warming of the matrix causes the trapped molecules to vibrate about their mean positions without their overall geometry being affected. Preferred orientation within the matrix may help to explain why NH_3^+ is rigidly trapped in the matrix whereas methyl radicals which would be expected to be of similar size are almost completely free to tumble in argon.

6.3 METHYL HALIDE EXPERIMENTS

When methyl iodide or methyl bromide argon mixtures were photolysed with argon resonance radiation during deposition, the methyl radical signal was increased dramatically as expected. Fine structure also appeared around the individual methyl lines. Figs 6.3 and 6.4 give the ESR spectrum obtained in these experiments using methyl bromide and methyl iodide. Clearly the spectrum obtained was dependent on the particular halide used. The experiment using methyl chloride produced just the expected methyl radicals.

Warming of the matrix produced large changes in the spectrum when CH_3Br was used as a substrate and only slight changes with CH_3I as a substrate. This difference in temperature dependence can possibly be explained by slight differences in the temperature dependence of the magnetic parameters between the species containing different isotopes of bromine. Annealing at 36 K simplified the spectra somewhat in both cases, the free methyl radical concentration increased relative to the new lines, although little real change was achieved. If Xenon resonance radiation (9.5, 8.4 eV [OKA78]) was used with CH_3Br the structure around the methyl lines was absent. The ionisation potential of CH_3Br is 10.6 eV [ROS77]. Addition of $(CH_2H_5)_3N$ which has an ionisation potential 7.5 eV [ROS77] to the CH_3Br mixture and photolysis with the Xenon lamp produced the same spectrum

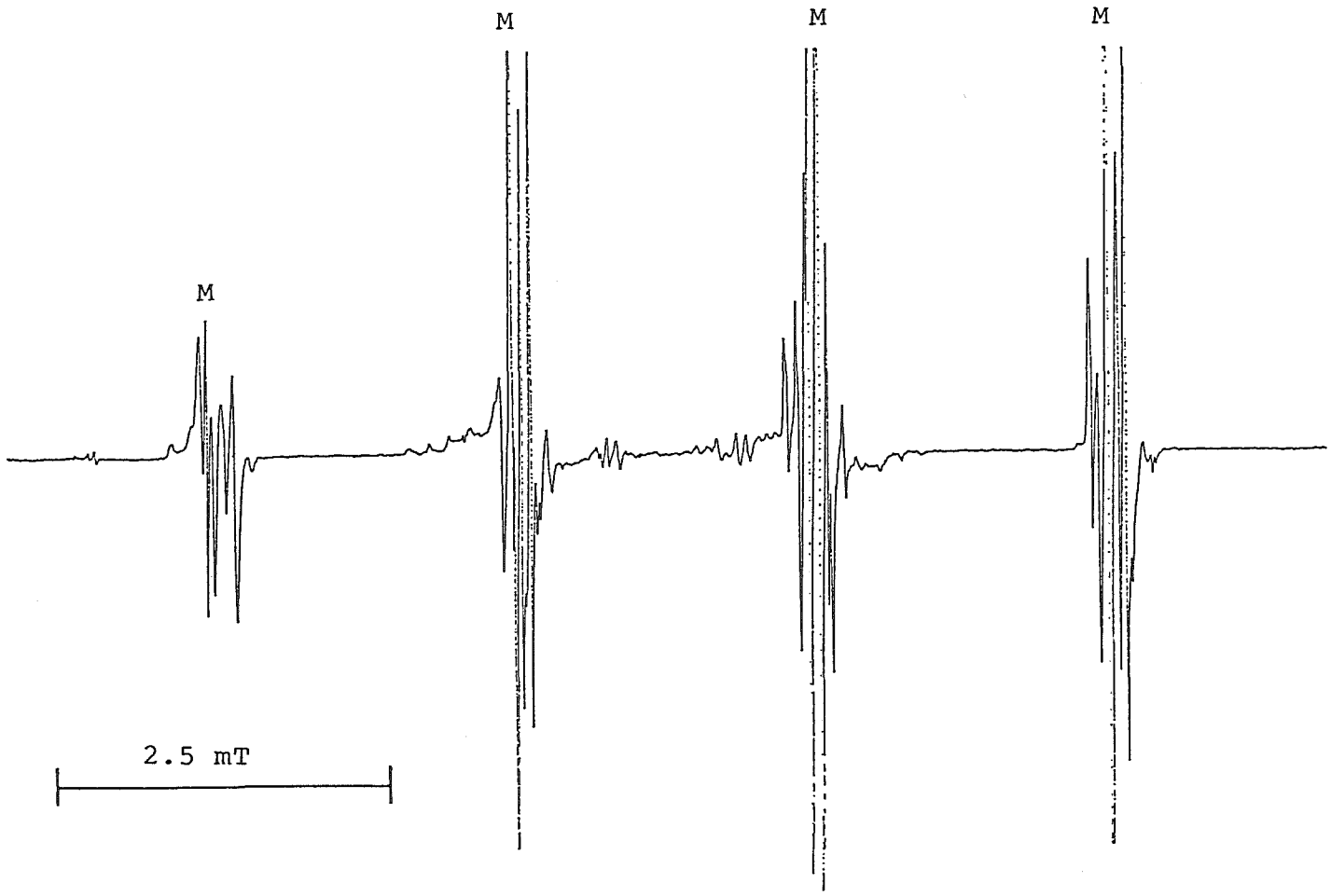

Fig. 6.3 ESR spectrum obtained at 12 K after methyl bromide argon mixture photolysed with argon resonance radiation during deposition. Assigned to $CH_3 \cdots Br^-$. Free methyl groups are marked M.

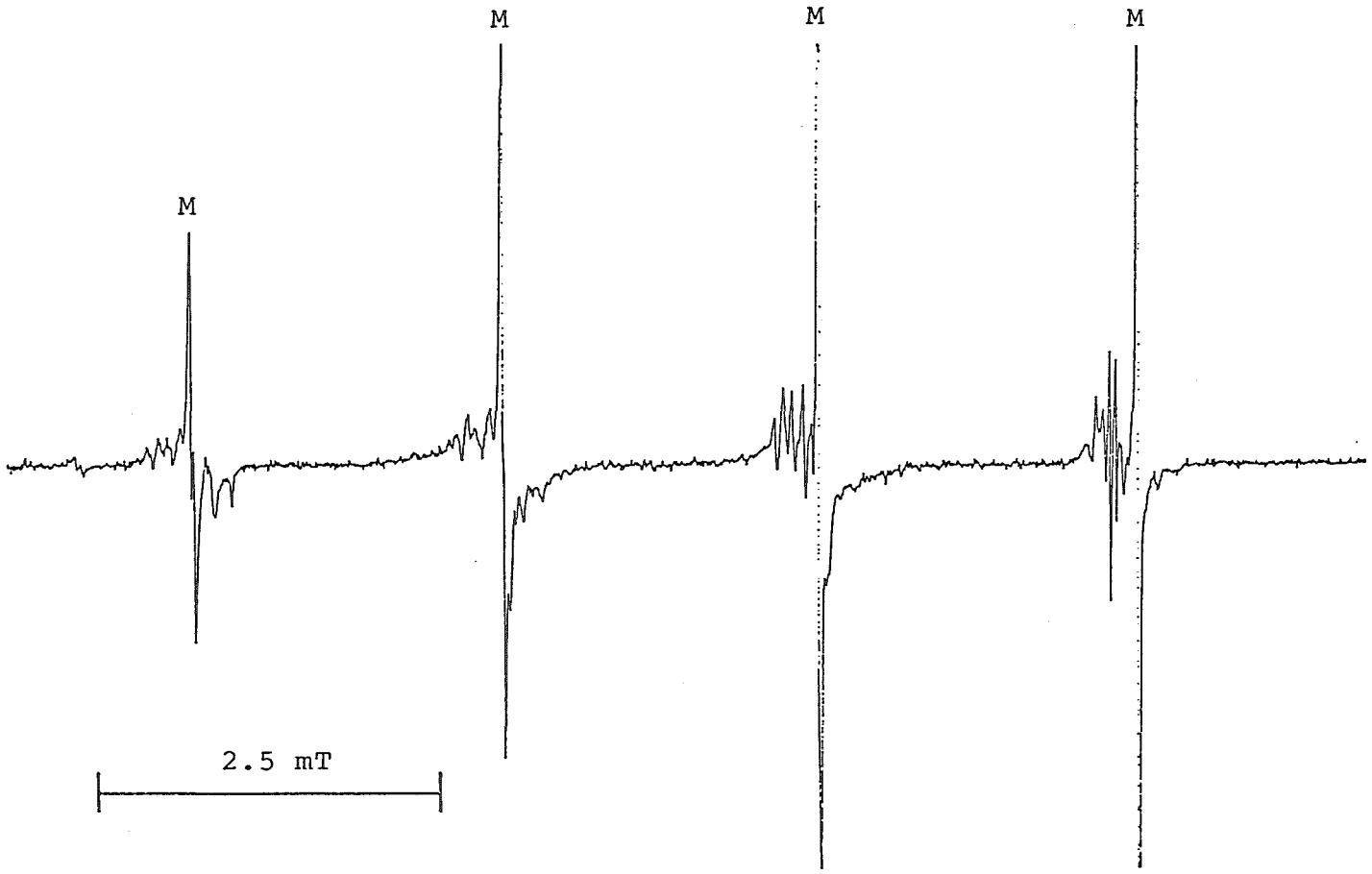

Fig. 6.4 ESR spectrum obtained at 12 K after methyl iodide argon mixture photolysed with argon resonance radiation during deposition. Assigned to $CH_3 \cdots I^-$. Free methyl groups are marked M.

as observed with argon resonance radiation. A blank with a $(CH_2H_5)_3N$ argon mixture produced only the background upon exposure to argon resonance radiation during deposition.

6.4 DISCUSSION OF METHYL HALIDE EXPERIMENTS

The species responsible for the structure around the methyl lines must be essentially a methyl radical as the spacing between the groups of lines is essentially unchanged. This methyl group must be interacting slightly with a nucleus or nucleii of high nuclear spin to produce the number of lines. The complexity of the spectrum points to the presence of more than one species. The interaction is known to be small as the coupling constant of the hydrogen atoms of the methyl radical is only reduced about 5 %. Electrons are known to be required for the production of this species and methyl chloride will not act as a precursor for this type of species.

Methyl iodide and methyl bromide are known to have a negative electron affinity. In other words upon electron capture, methyl iodide and bromide dissociate to produce methyl radicals and halide ions. Methyl chloride forms a stable negative ion. Symons et al. [SYM81] have observed the formation of radical anion pairs when methyl iodide or methyl bromide trapped in hard matrices such as acetonitrile at 77 K are subjected to gamma irradiation from a ^{60}Co source. It is known that one of the primary processes involved in gamma

irradiation is the production of electrons by the photo-electron effect. It therefore seems probable the species we observe trapped in argon, when methyl iodide or methyl bromide argon mixtures react with electrons during deposition, is a similar product. The degree of interaction is small and would be controlled by the spacing between the radical and the ion, which in turn would be controlled by the cage size of the host.

Symons et al [SYM81] have described the spectral characteristics of these radical ion adducts;

1) the spectra are centred about the free electron g value, and the high field lines are generally better resolved

2) if the halide ion interaction is isotropic the splitting constant is less than 1.0 mT

3) the hydrogen coupling constant is characteristic of the free alkyl radcial but is generally reduced between 5 and 10 %.

The species we observe in these experiments show all of the above characteristics.

We have been unable to solve the spectra of these species due to their complexity however in the methyl iodide

case it appears the hydrogen splitting constant is reduced by about 5 % to around 2.2 mT and the iodine splitting constant is around 0.05 mT. The reported isotropic splitting constants for the methyl radical-bromide ion and for the methyl radical-iodide ion adducts trapped in CD_3CN at 77K are 0.07 and -0.4 mT respectively. In both cases the methyl radical ion interaction is anisotropic. For an assignment of our observations to this type of species it appears necessary to conclude the methyl radical-ion interaction is isotropic, otherwise the loss of spin density from the methyl group could not be equated with the small halide splitting constants.

Symons et al. discuss the results of propyl-iodide radical ion adducts trapped in adamantane in terms of two sites, one isotropic with respect to the halide ion interaction and one anisotropic. Symons et al. suggest the isotropic case has the adduct trapped in two adjacent sites within the matrix and in the anisotropic case the adduct is trapped in one site. In acetonitrile matrices the adducts are always anisotropic implying one site for the adduct. The site size in argon would be smaller than in acetonitrile and would probably necessitate the adduct occupying two sites. This would explain the isotropic interaction with the halide ion we observe, as both parts of the adduct would be free to rotate independently and the anisotropic hyperfine interaction would be averaged out.

Experiments using deuterated methyl halides and a krypton matrix, to vary the cage size, were about to be begun when the turbo pump ceased to function.

6.5 ACETYLENE, ETHYLENE and DIACETYLENE EXPERIMENTS

Photolysis of acetylene, ethylene and diacetylene/argon mixtures during deposition with the argon resonance lamp produced C_2H radicals [COC64]. Elimination of hydrogen atoms from ethylene appears to be quite an efficient reaction as the major product of photolysis was not vinyl radical. There was no evidence of ions being produced in these experiments.

Warming of matrices containing acetylene produced a small level of a signal which was similar to a minor product of the photolysis of ethylene which is believed to be vinyl radical and is consistent with the observations of Kasai [KAI72] who performed similar experiments.

6.6 CARBON DISULPHIDE EXPERIMENTS

Bondybey et al. [BON79] have observed CS_2^+ trapped in argon matrices by Laser Induced Fluorescence. The CS_2^+ was formed by photolysis of existing CS_2 argon matrices with argon or hydrogen resonance lamps. This experiment has been repeated many times using photolysis from argon and krypton resonance lamps, during and after deposition upon

THE LIBRARY
UNIVERSITY OF CANTERBURY
CHURCH N.Z.

wide ranges of the concentration of CS_2 in argon. We have been unable to detect CS_2^+ trapped in argon in these experiments. The only product of these experiments was the normal background no other radical species seem to have been produced.

We believe our failure to observe CS_2^+ in these experiments was due to the far higher sensitivity of LIF over ESR. The CS_2^+ signal would also be expected to be quite anisotropic and this would further reduce the likelihood of detection.

6.7 HYDROGEN EXPERIMENTS

Hydrogen atom signals occurred in every photolysis experiment. The hydrogen atoms were trapped in two main sites following deposition. Multiple trapping of hydrogen atoms in argon has been discussed by Foner et al. [FON60] and later by Miyazaki et al. [MIY82]. Miyazaki et al. note the relative population of the sites is dependent on the energy of the ejected hydrogen. In our experiments the site which had the largest splitting constant was always the most intense upon deposition. This may indicate formation of the hydrogen atom prior to deposition although the excess energy involved with the hydrogen atom formation would always be higher than the experiments of Miyazaki. On annealing at 19 K the site with the smallest splitting constant was found to be most stable and its population increased slightly

during the annealing process. Further warming of the matrix reduced the hydrogen signal presumably due to recombination. During annealing at 19 K three minor sites were formed which did not always appear to be present immediately after deposition. Annealing at 28 K eliminated one of these minor sites. Fig 6.5 shows the low field lines of the hydrogen immediately after deposition and following annealing at 19 K and 28 K. The population of the minor sites varied from run to run but was always a few percent of the population of the major sites. In all the photolysis experiments the hydrogen atom signal was the most intense usually by a factor of one hundred.

6.8 HYDROGEN CYANIDE EXPERIMENTS

Photolysis of hydrogen cyanide argon mixtures with the argon lamp during deposition produced good yields of cyanogen radicals (CN·). The cyanogen radical spectrum was not completely isotropic, the $M_I^N = \pm 1$ lines were broader than the $M_I^N = 0$ line. Warming of the matrix caused the $M_I^N = \pm 1$ lines to reduce in linewidth until at 46 K the cyanogen spectra were essentially isotropic. During annealing a pair of lines as shown in fig 6.6 was observed under the $M_I^N = -1$ line of the cyanogen radical. These lines are obscured at 12 K due to the wide linewidth of the cyanogen radical. From 25 K upwards the cyanogen linewidth has decreased sufficiently to uncover this pair. This pair may indeed be a triplet with only the outside lines resolved

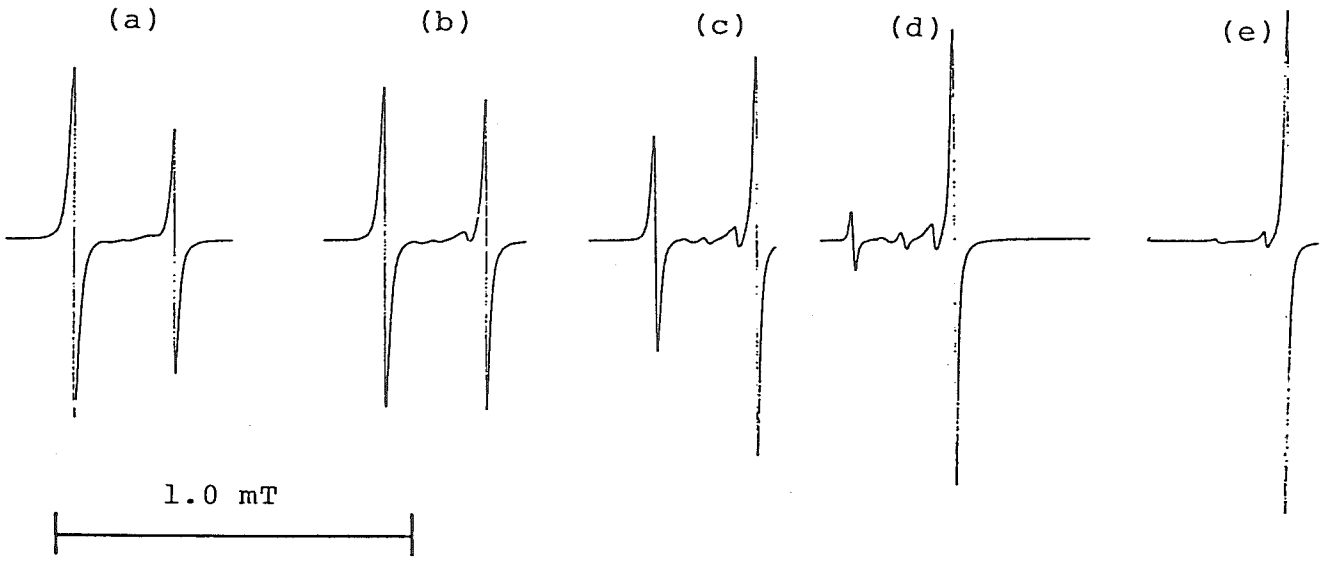

Fig. 6.5 Effect of temperature upon low field lines of hydrogen atoms in an argon matrix. All spectra were recorded at 13 K. (a) initial spectrum, (b) after annealing at 17 K for 1 min, (c) after annealing at 19 K for 2 mins, (d) after annealing for 20 mins at 19 K, (e) after annealing at 28 K for 10 mins.

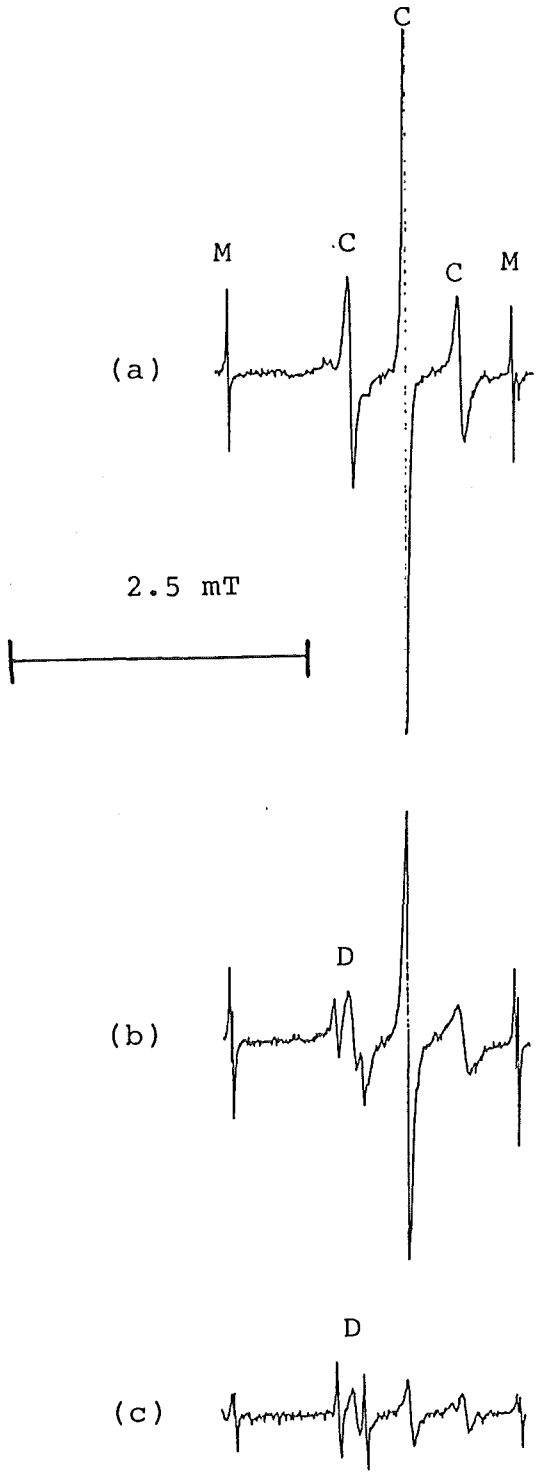

Fig. 6.6 Effect of temperature upon ESR spectrum obtained after hydrogen cyanide argon mixture photolysed with argon resonance radiation during deposition. (a) 12 K, (b) 26 K, (c) 38 K. M and C denote methyl and cyanogen radical. The doublet observed during annealing is marked D.

and the centre line covered by the cyanogen line. Returning the matrix to 12 K results in this pair being once more obscured as the cyanogen line broadens, and repeated annealing does not seem to increase the intensity of this pair. This implies the species responsible for this pair is not a reaction product formed during annealing of the matrix. The spacing of the pair is 0.53 mT and the g value relative to the cyanogen radicals [EAS70] is 2.008. The general behaviour of the cyanogen radical in these experiments is in good agreement with the published results [EAS70] . There was no evidence of rigidly trapped cyanogen radicals produced in our experiments. This is to be expected considering the high deposition temperature of 12K.

Experiments were tried with Deuterium Cyanide, prepared by the reaction of potassium cyanide and deuterated sulphuric acid. Similar results were obtained except that the $M_I^D = 0$ line of the deuterium atom obscured part of the unassigned pair. This experiment does not discount the species being responsible for the pair containing a hydrogen atom as the deuterium on deuterium cyanide would be very labile and therefore likely to be replaced by residual hydrogen in the apparatus as was the case with ND_3.

6.9 METHYL CYANIDE, METHYL ISOCYANIDE AND DICYANOGEN EXPERIMENTS

Argon mixtures of methyl cyanide and methyl isocyanide

produced only methyl radicals and hydrogen atoms when photolysed with a mercury resonance lamp (6.7 [OKA78]). The methyl lines except for the highest field line were found to be split. Argon resonance photolysis gave this same splitting of the methyl peaks and warming of the matrix to 30 K was found to have no irreversible effect upon this splitting. It appears likely this splitting is caused by multiple methyl sites in the matrix.

Upon argon resonance photolysis of methyl cyanide, methyl isocyanide and dicyanogen other broad resonance around g = 2 were observed. Cyanogen radicals were produced in good yield and also nitrogen atoms. In the dicyanogen case another clearly anisotropic intense resonance was observed in this region at g = 2.007 (relative to the cyanogen radical [EAS70]). Methyl cyanide and methyl isocyanide gave spectra containing similar but less intense resonances to the dicyanogen case and new features at g = 2.003 (relative to the cyanogen radical [EAS70]). These three spectra are given in figs 6.7, 6.8 and 6.9.

Infra-red spectroscopic investigation of the product of VUV photolysis of Methyl Cyanide and Methyl Isocyanide trapped in argon matrices by Jacox [JAC78a] has shown the presence of both CCN and CNC radicals. Loss of hydrogen atoms during photolysis in the matrix is a common phenomenon and is often the favoured result of VUV photolysis this is presumeably due to the high mobility of the hydrogen atom

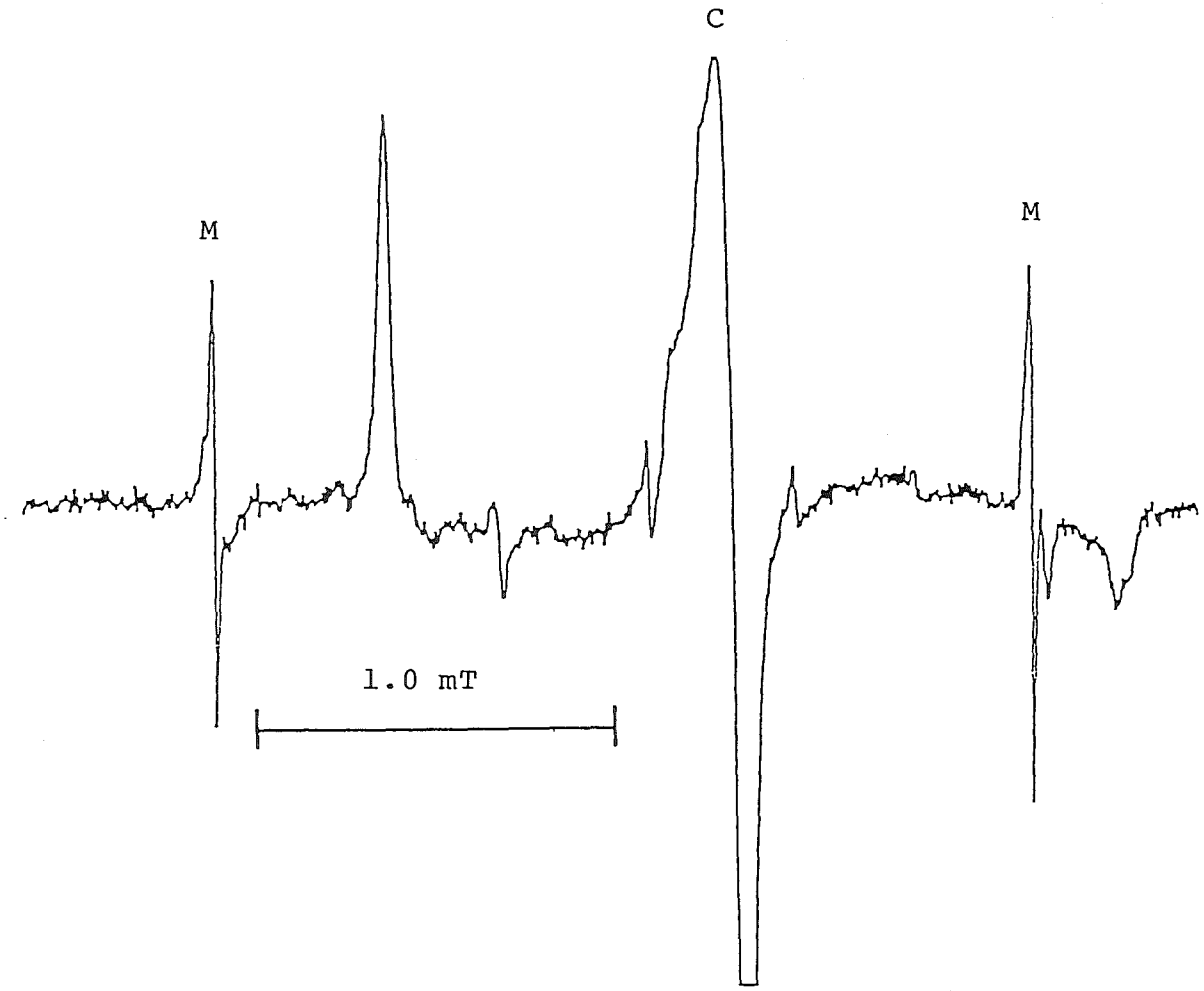

Fig. 6.7 The ESR spectrum recorded at 12 K obtained after a dicyanogen argon mixture was photolysed with argon resonance radiation during deposition. M methyl radical, C cyanogen radical.

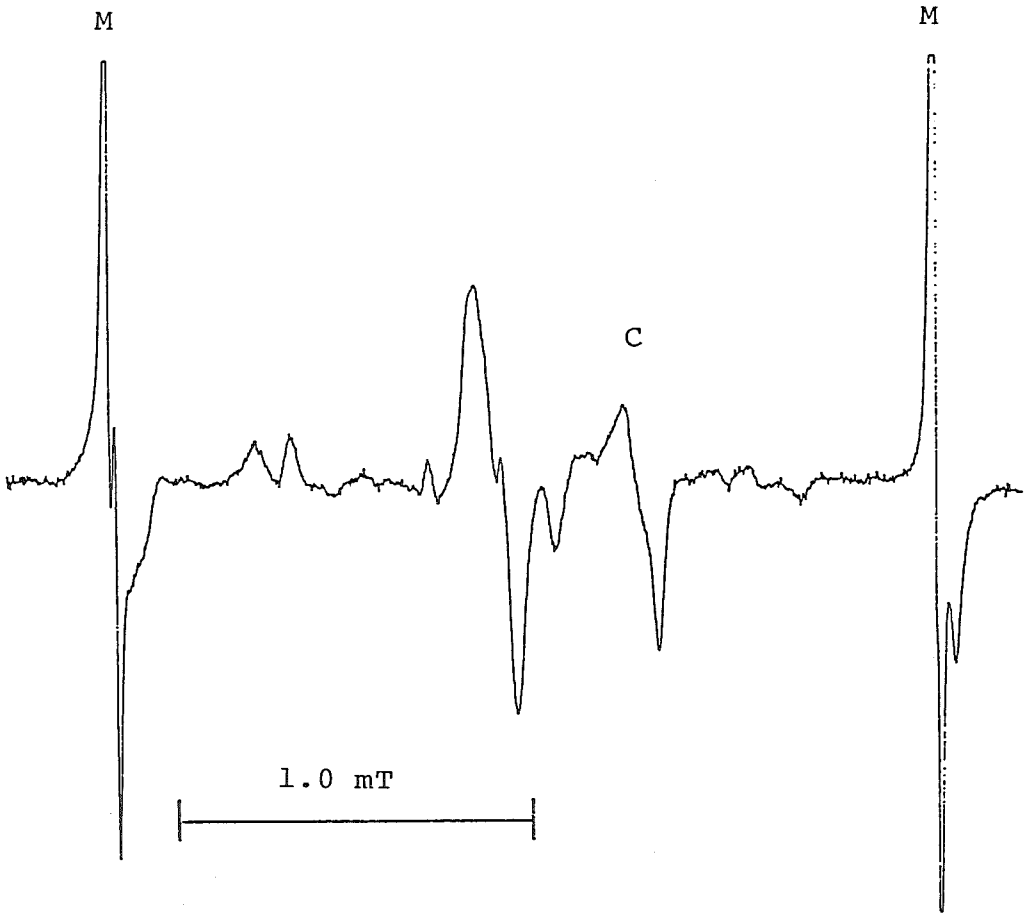

Fig. 6.8 The ESR spectrum recorded at 12 K obtained after a methyl cyanide argon mixture was photolysed with argon resonance radiation during deposition. M methyl radical, C cyanogen radical.

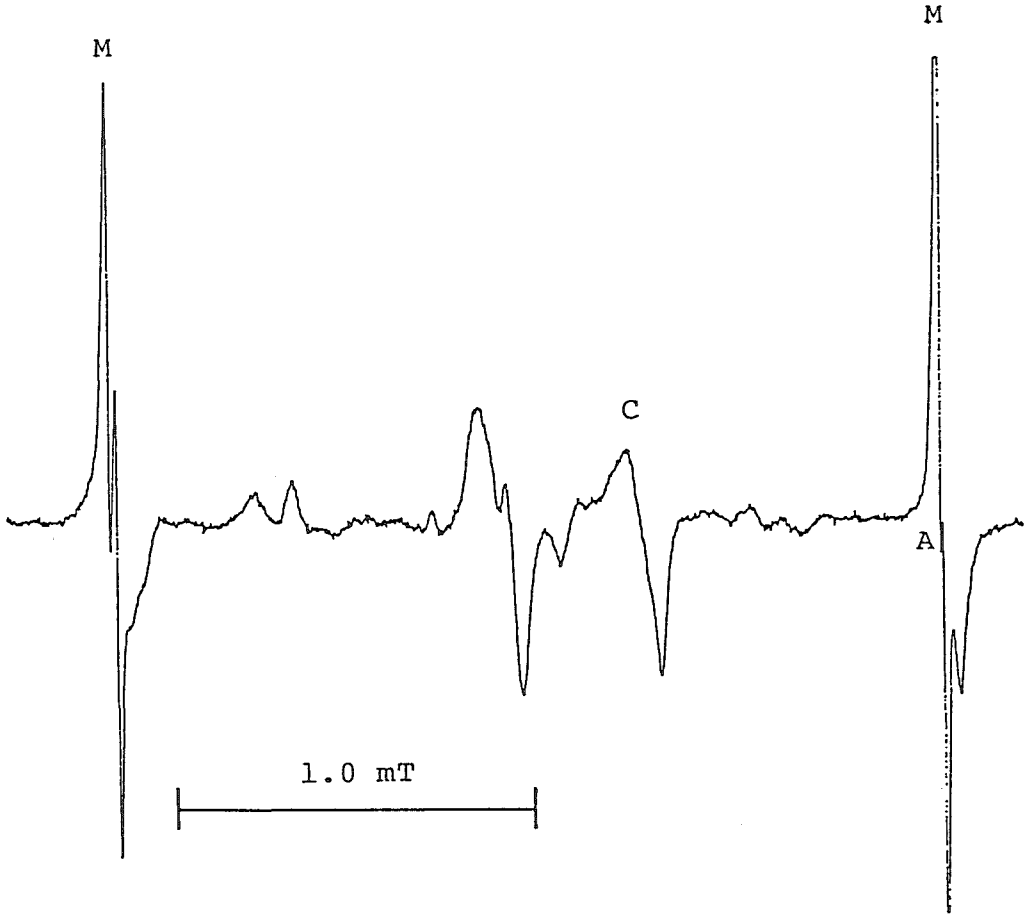

Fig. 6.9 The ESR spectrum recorded at 12 K obtained after a methyl isocyanide argon mixture was photolysed with argon resonance radiation during deposition. M methyl radical, C cyanogen radical, A instrumental artifact.

being such it can diffuse away from the other radical formed during photolysis. Larger radicals formed by photolysis being unable to separate in the matrix recombine.

The product observed with VUV photolysis of dicyanogen is most likely to be CCN in which case the major product with methyl isocyanide and cyanide is probably CNC. CH_2CN and similar species would be expected to give far wider resonances than observed due to the large interaction expected for the protons. CCN appears to predissociate [MER65] and reformation of the radicals would therefore favour CNC but this process would be expected to be independent of the substrate. It appears then this assignment would require some rearrangement of the substrate during or after absorption of the VUV photon.

These experiments exemplify the limitation of ESR when studying small radicals which are not free to rotate. Infra-red spectroscopy for example could give a far clearer picture of the products of these reactions.

7.0 MISCELLANEOUS EXPERIMENTS

Mixtures of the following compounds in argon were photolysed with the argon lamp and only the normal background species were produced:

bromine, chlorine, chloroform, triethylamine, sulphur dioxide, water, trifluoromethyl bromide, methane, carbon monoxide, carbon dioxide, dibromo-methane, ethyl bromide.

CHAPTER VII

CONCLUSION

The objective of this project was to trap small molecular ions in an argon matrix. To this end NH_3^+ formed by photoionisation of an argon ammonia mixture during deposition was observed by ESR trapped in an argon matrix.

Conventional electron impact ion sources had proved unsuitable for ion production in these experiments, presumably because of the energy of the resultant ions however experiments with a neon matrix and a quadrupole to focus and decelerate the ions could well prove productive [KNI83].

Radical ion adducts between methyl radicals and bromide or iodide ions appear to have been produced by photoionisation of either a methyl bromide or methyl iodide argon mixture during deposition. Similar experiments in a krypton matrix may help to confirm this assignment as the degree of interaction would be expected to be controlled by the host lattice dimensions. Possibly also isotopically enriched methyl bromide substrate could be used which would simplify the resulting spectra and allow their solution. Theoretical calculations could then be compared with the experimental data and may provide further insight

into the validity of the assignment. Other spectroscopic techniques, for example, far infra-red spectroscopy could produce further evidence of these adducts if the weak radical ion interaction could be observed.

ESR has proved to be a valuable technique with which to study radicals trapped in rare gas matrices but its usefulness is seriously reduced for radicals with small hyperfine interactions occurring around g = 2 owing to contamination of the matrix with radical impurities which also occurr at g = 2. Also for other than the smallest radicals, anisotropic spectra result which are difficult to solve and other spectroscopic techniques may be more appropriate.

APPENDIX I

CHEMICALS: SOURCE OR PREPARATION

(Fluoranthenyl)$_2^+PF_6^-$ (FlPF)

FlPF was synthesised by electrolysis of a CH_2Cl_2 solution of fluoranthene (BDH) and $N(Bu)_4^+PF_6^-$ at -30 ^oC using nickel electrodes. The $N(Bu)_4^+PF_6^-$ was prepared by reaction of $N(Bu)_4^+OH^-$, prepared by reacting aqueous $N(Bu)_4^+I$ (BDH) with Ag_2O (Ajax) followed by addition of $NH_4^+PF_6^-$ (Ventron) and extracting with CH_2Cl_2. The CH_2Cl_2 layer was dried with magnesium sulphate and the solvent evaporated. The CH_2Cl_2 (BDH) was purified by washing with concentrated sulphuric acid, and distilled. The electrolysis vessel was a U tube with a glass frit in the bottom. The electrodes which were flat disks were mounted through ground glass stoppers so that once in place the electrolysis cell was completely sealed from the atmosphere. It was found that electrolysis must proceed slowly (typical currents used were 0.05 mA for 6 days) and that the temperature had to be relatively constant at - 30 ^oC. Warmer temperatures and higher currents had been found to be unsatisfactory. A Townson and Mercer "Minus Seventy " temperature bath was used. The FlPF crystals were black lustrous rods and formed on the anode.

Matrix Isolation Experiments.

All gases used in these experiments, expect where impractical, were purified by several freeze-pump-thaw cycles and all liquids were purified by distillation under vacuum.

Acetylene: NZIG

Ammonia: Matheson

Ammonia D_3: reaction of Mg_3N_2 with D_2O

Ammonia ^{15}N: reaction of $Na^{15}NO_2$ (Merck Sharpe and Dohme) with Devarda's alloy in alkaline solution.

Argon: NZIG or UHP Matheson (see text)

Bromine: BDH

Carbon Dioxide: NZIG

Carbon Disulphide: BDH

Carbon Monoxide: CIG

Chlorine: Matheson

Chloroform: Ajax

Diacetylene: prepared after [ARM51]

Dibromo-Methane: BDH

Dicyanogen: Matheson

Ethyl Bromide: BDH

Ethylene: Matheson

Helium: NZIG

Hydrogen: NZIG

Hydrogen Cyanide: reaction of KCN and H_2SO_4

Hydrogen Cyanide D_1: reaction of KCN and D_2SO_4

Methane: Matheson

Methyl Bromide: BDH

Methyl Chloride: Virginia Chemicals

Methyl Cyanide: RDH

Methyl Iodide: M & B

Methyl Isocyanide: prepared after [CAS63]

Nitrogen: NZIG

Sulphur Dioxide: BDH

Sulphur Hexafluoride: Matheson

Triethylamine: BDH

Trifluoromethyl Bromide: Freon 13B1; Matheson

SUPPLIERS

Ajax c/- Smith Biolab P.B. Northcote, Auckland 9 N.Z.

British Drug House (BDH) P.O. Box 1246 Palmerston Nth. N.Z.

Commonwealth Industrial Gases (CIG) c/- NZIG

Matheson c/- NZIG

May and Baker (M & B) P.O. Box 35060 Nae Nae, Lower Hutt N.Z.

Merck Sharpe and Dohme (MSD) Isotope Division, P.O. Box 899,
Pointe Claire- Dorval, Quebec, Canada H9R 4P7.

New Zealand Industrial Gases (NZIG) P.O. Box 3020,
Lower Hutt. N.Z.

Riedal de Haen (RDH) c/- Scientific Supplies Ltd.,
21 Lorien Pl., East Tamaki, Auckland. N.Z.

Ventron Zeppelinstra e 7, Postfach 6540, D-7500, Karlsruche.
West Germany.

Virginia Chemicals Portsmount VA., USA.

APPENDIX II

CIRCUIT OF 2 kHz LOW PASS FILTER INSTALLED IN NMR GAUSSMETER

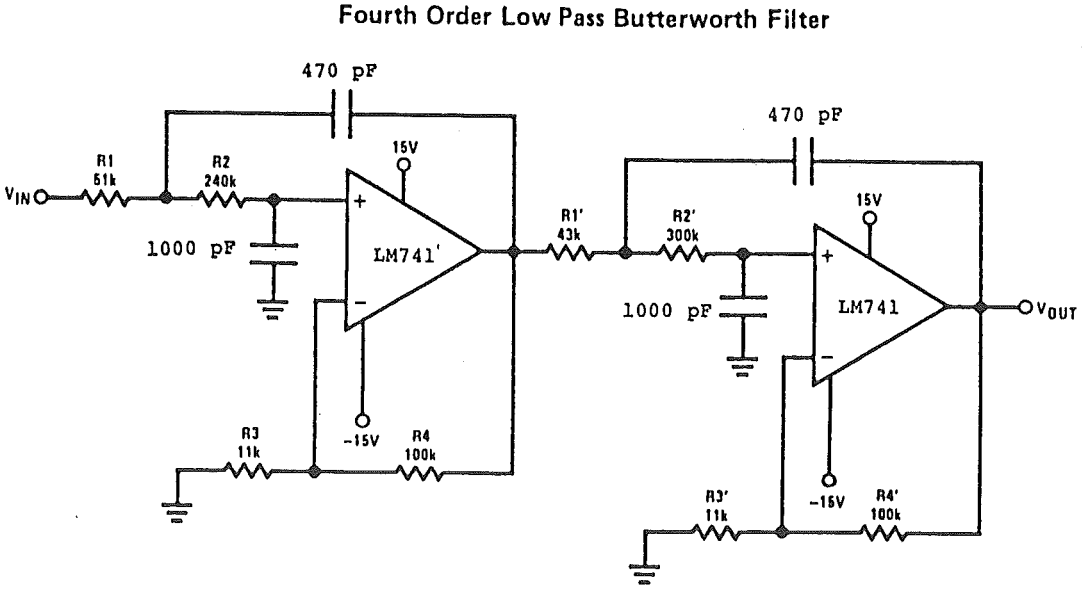

App. II Low pass filter incorporated in Y axis of NMR gaussmeter to remove noise caused by the computer. [National Semiconductor Applications Handbook 1982]

APPENDIX III

CIRCUIT OF THE THERMOCOUPLE AMPLIFIER

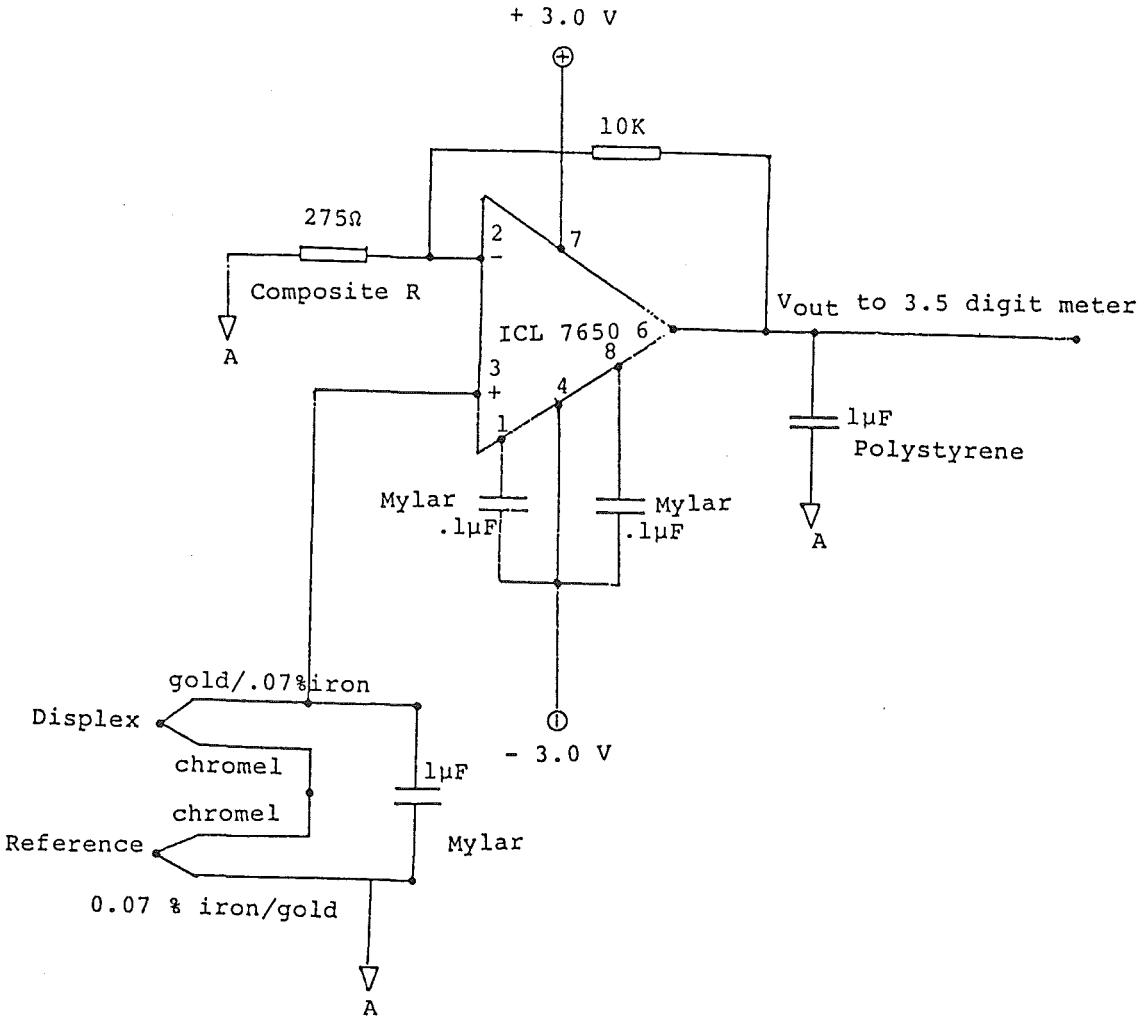

App. III Circuit diagram of thermocouple amplifier.

REFERENCES

AND68 Andrews, L. J. Am. Chem. Soc. 1968, 90, 7368.

AND73 Andrews, L.; Hwang, J.T.; Trindle, C. J. Phys. Chem. 1973, 77, 1065.

AND75 Andrews, L.; Grzybowski, J.M.; Allen, R.O. J. Phys. Chem. 1975, 79, 904.

AND79 Andrews, L. Ann. Rev. Phys. Chem., 1979, 30, 79.

ARM51 Armitage, J.B.; Jones, E.R.H.; Whiting, M.C. J. Chem. Soc. 1951, 44.

AUL75 Ault, B.S.; Andrews, L. J. Am. Chem. Soc. 1975, 97, 3824.

BAK85 Bakker, M.B. Ph.D. Dissertation, University of Canterbury, Christchurch, N.Z., 1985.

BAL62 Baldini, G. Phys Rev 1962, 128, 1562.

BAR81 Barnes, A.J.; Orville-Thomas, W.J.; Muller, A.; Gaufres, R.; Eds. "Matrix Isolation Spectroscopy"; Reidel: London, 1981.

BON79 Bondybey, V.E.; English, J.H. J. Chem. Phys. 1979, 71, 777.

BOX77 Box, H.C. "Radiation Effects"; Academic Press: New York, 1977.

BRA78 Bradley, J.N.; Metcalfe, E.M. Proc. R. Soc. Lond. A. 1978, 361, 367.

BRO66 Brown, S.C. "Introduction to Electrical Discharges in Gases"; John Wiley and Sons: New York, 1966.

BRU75 Brus, L.E.; Bondybey, V.E. J. Chem. Phys. 1975, 63, 3123.

BUT71 Butchard, J.A.; Claridge, R.F.C.; Phillips, L.F. Chem. Phys. Lett. 1971, 8, 139.

CAR67 Carrington, A.; McLachlan, A.D. "Introduction to Magnetic Resonance"; Harper and Row: New York, 1967.

CAS63 Casanova, J., Jr.; Schuster, R.E.; Werner, N.D. J. Chem. Soc. 1963, 4280.

CLA76 Claridge, R.F.C.; Weil, J.A. Unpublished data.

COC64 Cochran, E.L.; Adrian, F.J.; Bowers, V.A. J. Chem. Phys. 1964, 40, 213.

COC66 Cochran, E.L.; Adrian, F.J.; Bowers, V.A. J. Chem. Phys. 1966, 44, 4626.

COC69 Cochran, E.L.; Adrian, F.J.; Bowers, V.A. J. Chem. Phys. 1969, 51, 2759.

COL61 Cole, T. J. Chem. Phys. 1961, 35, 1169.

EAS70 Easley, W.C.; Weltner, W., Jr. J. Chem. Phys. 1970, 52, 197.

EXN75 Instruction Manual for Extranuclear Laboratories Inc. Electron Impact Ioniser Model 041-3.

FIT70 Fitch, R.K.; Mulvey, T.; Thatcher, W.J.; McIlraith, A.H. J. Phys. D: Appl. Phys. 1970, 3, 1399.

FON60 Foner, S.N.; Cochran, E.L.; Bowers, V.A.; Jen, C.K. J. Chem. Phys. 1960, 32, 963.

FRA77 Frait, Z.; Gemperle, R. Czech. J. Phys. B 1977, 27, 99.

HYD61 Hyde, J.S.; Freeman, E.S. J. Phys. Chem. 1961, 65, 1636.

JAC78 Jacox, M.E. Rev. Chem. Intermed. 1978, 1, 1.

JAC78a Jacox, M.E. J. Mol. Spect. 1968, 71, 369.

KAI68 Kasai, P.H. Phys. Rev. Lett. 1968, 21, 67.

KAI72 Kasai, P.H. J. Am. Chem. Soc. 1972, 94, 5950.

KAI71 Kasai, P.H. Acc. Chem. Res. 1971, 4, 329.

KEL82 Kelsall, B.J.; Andrews, L. J. Chem Phys. 1982, 76, 5005.

KHO77 Khorossany, M.; Fitch, R.K. Vacuum 1977, 27, 159.

KNI82 Knight, L.B., Jr.; Steadman, J. J. Chem. Phys. 1982, 77, 1750.

KNI83 Knight, L.B., Jr.; Bostick, J.M.; Woodward R.M.; Steadman, J. J. Chem. Phys. 1983, 78, 6415.

KNI83a Knight, L.B., Jr. Personal communucation.

KNI83b Knight, L.B., Jr.; Steadman, J. J. Chem. Phys. 1983, 78, 5940.

KNI84 Knight, L.B., Jr.; Miller, P.K.; Steadman, J. J. Chem. Phys. 1984, 80, 4587.

MCI66 McIlraith, A.H. Nature (London) 1966, 212, 1422.

MER65 Merer, A.J.; Travis, D.N. Can. J. Phys. 1965, 43, 1795.

MIL69 Milligan, D.E.; Jacox, M.E. J. Chem. Phys. 1969, 51, 1952.

MIL70 Milligan, D.E.; Jacox, M.E.; Guillory, W.A. J. Chem. Phys. 1970, 52, 3864.

MIY82 Miyazaki, T.; Wakahara, A.; Usul, T.; Feuli, K. J. Phys. Chem. 1982, 86, 3881.

MOT72 Mothes, K.G.; Schultes, E.; Schindler, R.N. J. Phys. Chem. 1972, 76, 3758.

MUL52 Mulliken, R.S. J. Phys. Chem. 1952, 56, 801.

OKA78 Okabe, H. "Photochemistry of Small Molecules"; Wiley- Interscience: U.S.A., 1978.

PEA76 Pearse, R.W.B.; Gaydon, A.G. "The Identification of Molecular Spectra"; 4th Ed., Chapman and Hall: London, 1976.

PER75 Perlson, B.D.; Weil, J.A. Rev. Sci. Instrum. 1975, 46, 874.

PER85 Perutz, R. N. Chem. Rev.1985, 85, 1;

Perutz, R. N. Chem. Rev.1985, 85, 97.

POO83 Poole, C.P. "Electron Spin Resonance"; John Wiley and Sons: New York, 1983.

ROS77 Rosenstock, H.M.; Draxl, K.; Steiner, B.W.; Heron, J. J. Phys. Chem. Ref. Data 1977, 6, Supplement No. 1.

RUS71 Rushton, G.J.; Fitch, R.K. Vacuum 1971, 21, 449.

RUS73 Rushton, G.J.; O'Shea, K.R.; Fitch, R.K. J. Phys. D 1973, 6, 1167.

SAC82 Sachs, G.; Stocklein, B.; Dormann, E.; Schwoerer, M. Chem. Phys. Lett. 1982, 89, 179.

SPI62 Spindel, W. In "Inorganic Isotopic Synthesis"; Herber, R.H., Ed., W.A. Benjamin: New York, 1962.

SYM81 Symons, M.C.R.; Smith, I.G. J. Chem. Soc., Perkin Trans. 2, 1981, 1180.

VRE74 Vreede, H.J.; Claridge, R.F.C.; Phillips, L.F. Chem. Phys. Lett. 1974, 27, 1.

LIST OF FIGURES

Title

ACKNOWLEDGEMENTS

I wish to thank my supervisors Dr R.F.C. Claridge and Dr P.W. Harland for their help and encouragement during the course of this project. I also wish to thank the technical staff in this department for their help and co-operation, and thank Dr M.G. Bakker for many informative discussions.